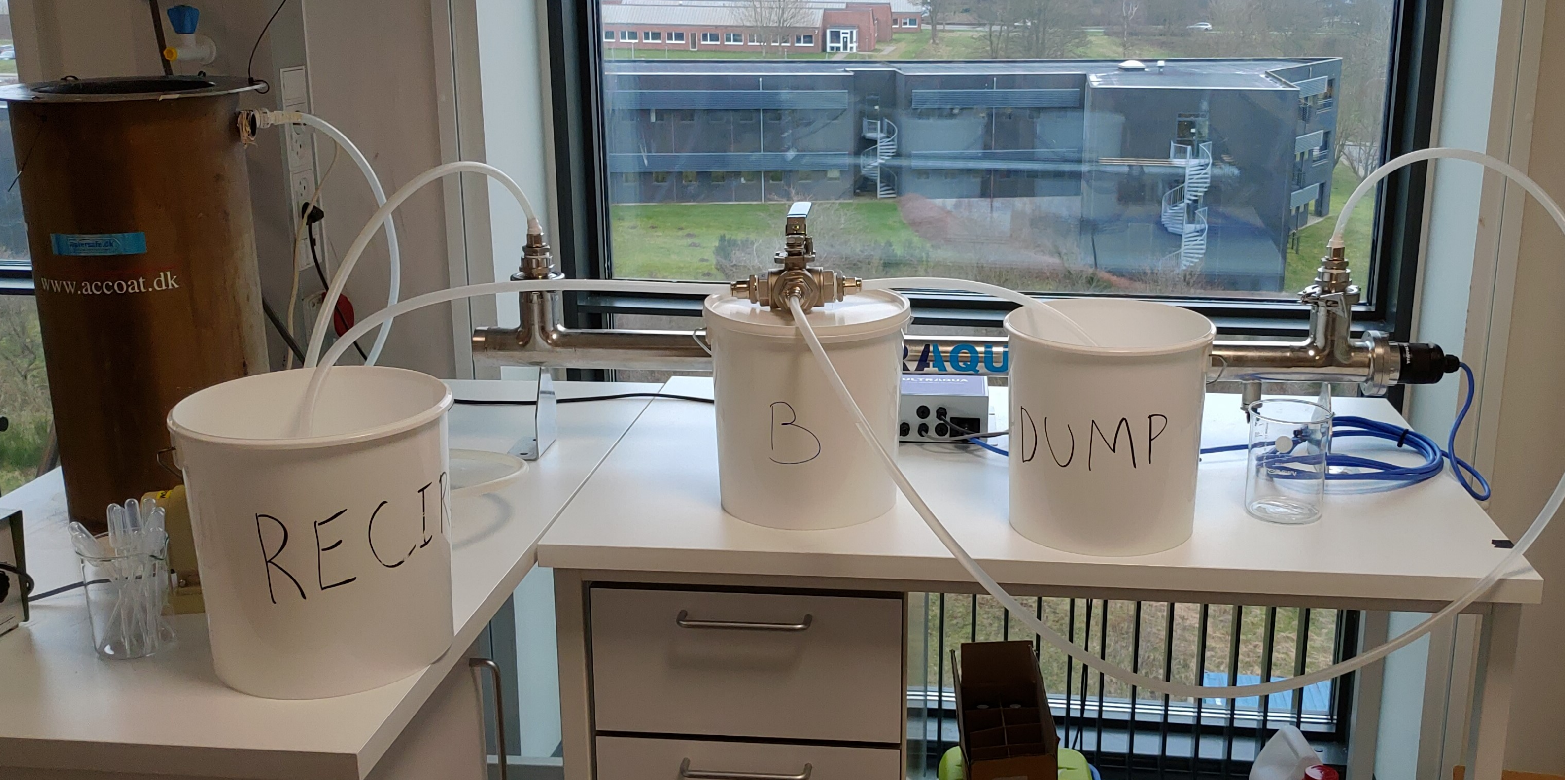

Kinetic modeling and rate constant determination of Vacuum-UV oxidation of BAM in Danish groundwater

Lars Breinholt

Chemical Engineering, Jun. 2020

Master's Thesis

Title	Kinetic modeling and rate constant determination of Vacuum-UV oxidation of BAM in Danish groundwater
Field of study	Chemical Engineering
Location	Aalborg University Esbjerg
Supervisors	Jens Muff & Morten E. Simonsen

Lars Breinholt

Lars Breinholt

Abstract

The degradation of 2,6-dichlorobenzamide (BAM) in a Vacuum-UV (VUV) reactor was kinetically modeled. The reactor was provided by Ultraaqua, and had a volume of 1.74 L and used a low-pressure mercury lamp with an emission at 185 nm. The $OH^{\bullet}$ rate constant for BAM determined experimentally using competition kinetics, and theoretically using a group contribution method. The two methods yielded similar results, $2.34 \cdot 10^9$ $M^{-1}\,s^{-1}$ for the experimental method and $4.88 \cdot 10^9$ $M^{-1}\,s^{-1}$ for the theoretical.

Degradation of BAM in groundwater from Esbjerg was modeled in 1 $mg\,L^{-1}$ scale to investigate scavenging effects. Bicarbonate and NVOC scavenged $OH^{\bullet}$ similarly, while chloride and bicarbonate absorbed the majority of the radiation, with chloride absorbing 5 times as much as bicarbonate.

In groundwater scale the effect of multiple pesticides and different water compositions were modeled. In Esbjerg water less than one pass through the reactor was needed to degrade BAM below the threshold, with an initial concentration in the range 0.2-0.5 $\mu g\,L^{-1}$, independent of the rate constant used. Addition of 2-methyl-4-chlorophenoxy acetic acid (MCPA) was done to simulate the effect of multiple pesticides. An addition of at least 100 $\mu g\,L^{-1}$ was needed to noticeably inhibit BAM degradation. Water from Middelfart and Hvidovre was simulated and compared with water from Esbjerg. The equivalent reactors needed to degrade 0.5 $\mu g\,L^{-1}$ below the threshold increased from 0.33-0.65 in Esbjerg water, depending on rate constant, to 0.71-1.53 in Middelfart water and 1.90 to above 4 in Hvidovre water.

The difference in degradation was also reflected in energy consumption, where the electrical energy-per-order needed in Esbjerg water was 0.69-1.49 $kW\,h\,m^{-3}\,order^{-1}$ compared to the higher values for Middelfart water, 1.56-3.28, and Hvidovre water, 4.12-8.69.

Preface

This study took place from 01/02-2020 to 04/06-2020 by Lars Breinholt, in the department of Chemical Engineering at Aalborg University Esbjerg. As this project was performed during the COVID-19 pandemic, the scope of the project was changed partway through, which eliminated further experimental work after the 18th of March. Thus, the majority of this project is focused on theoretical work.

A special acknowledgement goes to my supervisors Jens Muff and Morten E. Simonsen for their guidance, and Peter V. Christensen and Morten M. Klausen from Ultraaqua, for providing the Vacuum-UV reactor and additional guidance.

Contents

Nomenclature

Abbreviations

AOP	Advanced Oxidation Processes
BAM	2,6-dichlorobenzamide
DMS	N,N-dimethyl-sulfamide
DPC	Desphenylchloridazon
GCM	Group Contribution Method
LP Hg	Low-pressure mercury
LSPP	Line source model with parallel plane emission
LVRPA	Local volumetric rate of photon absorption
MCPA	2-methyl-4-chlorophenoxy acetic acid
MCPP	2-methyl-4-chlorophenoxypropionic acid
MDPC	Methyldesphenylchloridazon
NOM	Natural organic matter
NVOC	Non-volatile organic carbon
PFR	Plug-flow reactor
RNO	4-nitrosodimethylaniline
SSA	Steady-state approximation
UV	Ultraviolet
UV/Vis	Ultraviolet-visble
VRPA	Volumetric rate of photon absorption
VUV	Vacuum ultraviolet

Symbols

α	Napieran absorption coefficient, m^{-1}; also used for the first carbon attached to a functional group
β	Second carbon attached to a functional group
ϵ	Molar absorption coefficient, $M^{-1}\,cm^{-1}$ or $M^{-1}\,m^{-1}$
Φ	Quantum yield, $mol\,einstein^{-1}$

A	Absorption coefficient m^{-1} or cm^{-1}; also preexponential factor, M^{-1} s^{-1}, and absorbance, dimensionless
C	Concentration, mol L^{-1}
E_a	Activation energy, J
E_{EO}	Electrical energy-per-order, kW h m^{-3} order^{-1}
F	Molar flowrate, M s^{-1}
I	Irradiance, W m^{-2}
k	Rate constant, unit varies, generally M^{-1} s^{-1}
$k^{'}$	Apparent rate constant, s^{-1}
L	Lamp arc length, m
P	Electrical input, kW
P_{VUV}	Power of the 185 nm emission, W
Q	Volumetric flowrate, L min^{-1} or m^3 h^{-1}
R	Reaction rate, M s^{-1}; also ideal gas constant 8.314 J mol^{-1} K
r	Radial coordinate, m
R_q	Quartz sleeve radius, m
R_r	Reactor radius, m
S	Loss rate, s^{-1}
T	Temperature, K
V	Volume, L
$X\text{-}Z_R$	Functional group factor, dimensionless
x_λ	Fractional photon absorption, dimensionless

1. Introduction

In recent years, the pesticide pollution of Danish groundwater have become apparent. New analytical methods means that many more pesticides are detectable and the detection limit has decreased. This has meant a larger number of groundwater wells have been identified as pesticide polluted. After the introduction of the latest analytical methods, more than 75 new pesticide pollutants have been discovered in groundwater, and more than 40% of groundwater wells have been found to be polluted [1, 2]. This is a problem, as groundwater is the primary source of drinking water in Denmark.

A wide variety of pesticides are polluting the groundwater, and the analytical methods have greatly influenced, what pesticides are found in the highest quantity. Earlier it was the degradation product 2,6-dichlorobenzamide (BAM) and phenoxy acid herbicides, that were found in the highest quantities. Today, BAM is still one of the major polluters, together with the more newly discovered pollution of, the two degradation products of chloridazon, 1,2,4-triazol and N,N-dimethyl-sulfamide (DMS). DMS especially is a problem, and has resulted in temporary shutdown of two waterworks [3], and is still found in the drinking water, diluted to below the threshold, for approximately 400,000 people.

Only limited treatment is performed on drinking water in Denmark, as the groundwater has a generally high quality. Drinking water treatment only includes aeration, and sand-filtration of Mg^{2+} and Fe^{2+}, and treatment beyond this is only allowed with a time limited permit. The only treatment method allowed for treatment of pesticides is currently using activated carbon filtration, and this has only been approved in treatment of BAM. UV treatment has generally only been approved for disinfection, however it has also been approved together with activated carbon for treatment of BAM [4]. Advanced treatment is generally only allowed if the waterwork have no other option, which means, that in most cases a polluted well results in closing the well, and finding water elsewhere.

This study investigates modeling of Vacuum-UV (VUV) irradation as an advanced oxidation process (AOP) for drinking water treatment of pesticides. Background knowledge of pesticide pollution in Denmark, and VUV technology will be presented, together with state-of-the-art research on degradation of organic pollutants using VUV and modeling of photoreactors. The main advantage of the VUV system, is the possibility for a fully homogeneous system without use of chemicals, which decreases the cost in both operation and materials. The process is also not selective, meaning that it can be used for treatment of any type of organic pollutant, including all pesticides.

2. Pesticide pollution

2.1 Pesticides

Pesticides is a term for chemicals used for controlling pests, including fungicides, herbicides, insecticides among others. These have been very influential in increasing the effectiveness of farming by reducing loss due to insect, parasitic fungi, competing plants etc. In Europe and USA the estimated crop losses without pesticides are 10-30%, but in some developing countries this estimation have been reported as high as 75% [5].
While pesticides are very useful for removing pests in agriculture, this characteristic also mean, that they are generally toxic for humans. This is not immediately of concern, but after use, the pesticides can, over time, leach through the soil down into the groundwater. As Denmark sources all of its drinking water from groundwater this pollution is a potential problem. Pesticides are normally used by spraying an aerosol of the pesticides over the crops. The pesticides can then leach through the soil together with rain. The top soil layer can, in some cases, help with degradation of the pesticides by microorganisms. However, this depends on the amount of organic material and clay minerals, and the pesticides' affinity for adsorption to these. This means that some pesticides are either not degraded at all or only partially degraded into a its degradation product, with in some cases can be more toxic. Heavy rain can also increase the leaching rate, leading to lower pesticide degradation [6].
The leaching of pesticides to the groundwater is a slow process and it takes many years before they are found in the groundwater. Regulations against pesticides, were as such, first made in the 1980's when the pollution was discovered. The regulations made both ban the use specific pesticides and the amount of pollution allowed in drinking water. **Table 1** shows the thresholds for pesticides in drinking water. The threshold was at the time, chosen to be the detection limit, to prevent any amount of pesticides or their degradation products in drinking water. The threshold also includes a limit, for the sum of all pesticides. In practice, if the sum threshold is broken, the single pesticide threshold is broken as well. The lower threshold for the four specific pesticides was chosen based on a health assessment [6–8].

Table 1: Pesticides and their threshold [9].

Pesticide	Threshold ($\mu g\,L^{-1}$)
Aldrin, dieldrin, heptachlor, heptachlorepoxid	0.030
Other pesticides	0.10
Sum of all pesticides	0.50

2.2 Drinking water pollution

While many of the most harmful pesticides have been banned for a long time, due to the quantities already used, most of the pesticides and degradation products found in groundwater, are from banned pesticides. As such, the ban on harmful pesticides was a reactive action to limit further pollution. The groundwater was monitored in the period of 1992-2017, both by the individual waterworks, but also as part of a nationwide groundwater monitoring. **Figure 1** shows the findings from 2013-2017, from the waterworks monitoring. This shows that the problem is nationwide, with pollution shown by the blue and red dots. This monitoring included new analytical methods, which included more pesticides detectable and lower detection limits. This has resulted in finding a larger amount of wells to be polluted. With the new analytical methods, more than 40% of groundwater wells was found to be polluted, and more than 75 new pollutants was found [1, 2]. The groundwater and waterworks monitoring identified a number of pesticides, which threatens the drinking water. Before the newer analytical methods, some of the most observed pollutants were BAMf and phenoxy acids. BAM especially is still one of the largest pollution in groundwater wells. BAM is the degradation product of dichlobenil, which was sold in the two herbicides Prefix and Casoron, and used in the period 1965-1997 until it was banned. The phenoxy acids herbicides covers a

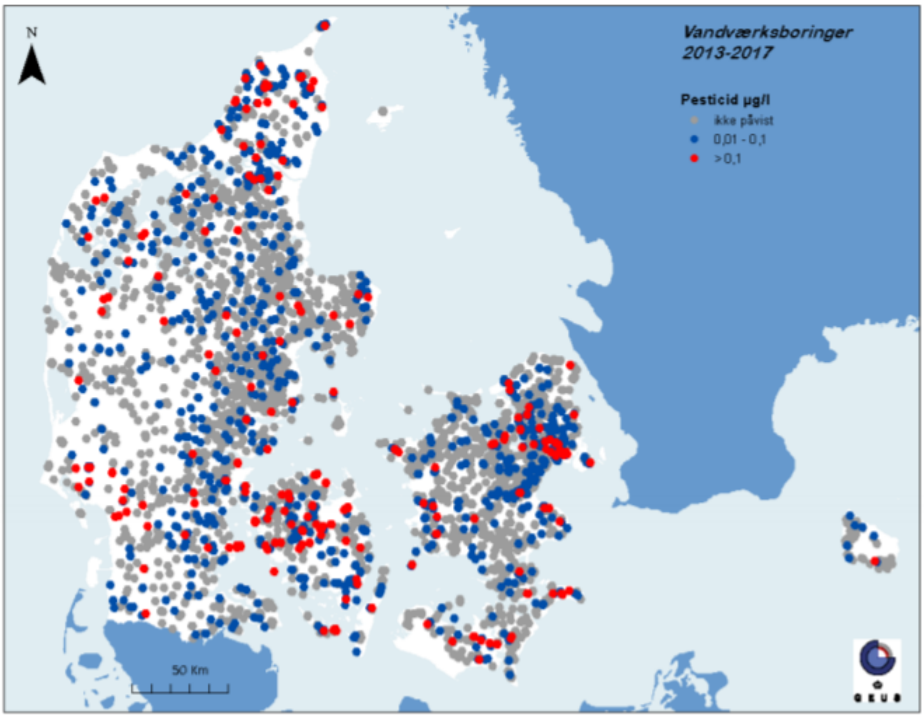

Figure 1: Waterworks monitoring of pesticides. Grey dots mean no pesticides found, blue mean pesticides found below the threshold (0.01 - 0.1 $\mu g\,L^{-1}$) and red dots mean pesticides found above the threshold (>0.1 $\mu g\,L^{-1}$). Reprinted from Thorling et al. [8] available at `www.grundvandsovervaagning.dk`.

handful of different pesticides, including 2-methyl-4-chlorophenoxy acetic acid (MCPA) and 2-methyl-4-chlorophenoxypropionic acid (Mechlorprop or MCPP). Phenoxy acids have been used in large quantities, in the period of 1963-2004, 29500 tons were used. The phenoxy acids have since been either banned or regulated, and the usage has significantly decreased.

The most polluting pesticides included in the new analytical methods include the degradation products of chloridazon, 1,2,4-triazol and N,N-dimethylsulfamide (DMS). Chloridazon was in use in the period of 1964-1996, and its two degradation products, desphenylchloridazon (DPC) and methyldesphenylchloridazon (MDPC) are now two of the most found pollutants. In waterwork monitoring, they were found first and third most, while in the groundwater monitoring they were found second and third most, with DPC being found most often between the two. 1,2,4-triazol is a degradation product of several triazol fungicides and tt was found most in the groundwater monitoring, but was not analysed for in the waterworks monitoring. Lastly, DMS was not analysed for in either the groundwater or waterworks monitoring, however in an analysis in 2018, DMS was found in 47% of 51 samples from different waterworks. DMS is the degradation product from tolylfluanid and dichlofluanid, which were in use in the period 1973-2007.
In this study, BAM was used as a model pollutant, as it is both found in large amount of groundwater wells and previously studied. The structure of BAM is shown in **Figure 2**.

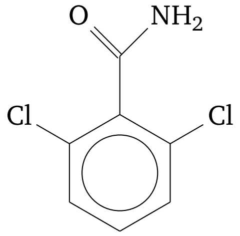

Figure 2: The molecular structure of BAM.

2.3 Current Approach

In Denmark, treatment of drinking water is only allowed with a limited permit. Generally, if a groundwater well is polluted, it is abandoned and drinking water must be found elsewhere. This could prove to be an unsustainable method, with the newer analytical methods discovering more pesticides, in lower concentration. The other option is treatment, however, only activated carbon filtration has so far been granted permission to use against pesticide polluted groundwater [4] This method can be fairly ineffective at filtrating more polar molecules. The activated carbon filtration has only been used for cleaning water polluted with BAM, and as BAM is a polar molecule, which is more hydrophilic, this increases the cost, as the filter needs to be changed more often. This current approach, is then, either ineffective or unsustainable. This has lead to more than 1300 wells being closed before 2005 and some waterworks resorting to diluting the water, to stay below the threshold [6, 10]. If this problem persists, it necessitates change, either an increase in threshold levels, or other forms of treatment used. This has lead to more treatment options being researched, such as using membranes [11], or a combined membrane and biological treatment [12]. While the combined treatment option solves the problem of cleaning the retentate from the membrane, some pesticides, such as BAM can only be degraded by a certain bacteria, which could be a problem, with all the different pesticides found. Advanced oxidation processes are less selective, and as such could be more suitable, given the amount of different pollutants found. There are many different AOPs, however, most suitable are the ones that rely on radicals, as they both have high reduction potentials and are highly reactive. The two main radicals are the hydroxyl radical ($OH^{\bullet}$) with a reduction potential of 2.7 V, and the sulphate radical ($SO_4^{-\bullet}$) with a reduction potential of 2.5 V [13]. These can both be generated chemically, however addition of chemicals can be expensive. Other methods include photochemical and electrochemical methods, of which the latter can be combined with the activated carbon filters. For photochemical methods, the most studied are UV/H_2O_2 and heterogeneous photocatalysis, using UV light and titanium dioxide. However, if a lower wavelength UV light is used, below 200 nm, water itself can absorb the radiation and form hydroxyl radicals. This system has the advantage of being both a chemical free and homogeneous system. This greatly reduces complexity, as all that is needed is a lamp emitting the low wavelength UV, Vacuum-UV light [14].

3. Vacuum-UV irradiation

The low wavelength, high energy VUV radiation are generally achieved using one of the two most common lamp types: low-pressure mercury lamp (LP Hg) with an emission at 185 nm or excimer lamps, generally using Xenon, with an emission at 172 nm. The LP Hg lamp is the most common. The LP Hg lamp emit monochromatic radiation and has two emissions, at 184.9 and 253.7 nm. This is achieved by Hg or amalgam at 1 Pa, which corresponds to a vapour pressure of 40°C [14, 15]. The intensity of the 185 nm emission is lower, at about 25% of the 254 nm emssion. To make use of the VUV radiation, special high purity quartz glass is also needed, as regular glass does not transmits the low wavelength. fThe 185 nm radiation is strongly absorbed by water, which means the penetration is very low. The absorption coefficient of 185 nm radiation in water is in the range 1.46-1.80 cm^{-1}, and the majority of the radiation is absorbed within a few millimeters [14–18].

3.1 Generation of hydroxyl radicals

The absorbance of the VUV radiation by water, is the source of the hydroxyl radicals. This absorbance leads to a photolysis of water, which can affect it in two ways: homolysis (1), which splits it into the hydroxyl and hydrogen radical, or photochemical ionization (2), which instead produces a hydrogen ion and a solvated electron. The homolysis is favoured, shown by the higher quantum yield [14–16, 19–21].

$$H_2O + hv(185\text{ nm}) \longrightarrow OH^{\bullet} + H^{\bullet} \qquad \Phi = 0.33 \quad (1)$$

$$H_2O + hv(185\text{ nm}) \longrightarrow OH^{\bullet} + H^{+} + e^{-}_{aq} \qquad \Phi = 0.045 \quad (2)$$

While the high reactivity of radicals, due to their unpaired electron, is useful for faster degradation, their instability also means that they are not selective. The low selectivity means that the hydroxyl radicals can react with other types of organic matter, some types of minerals, and also other radicals. The radical reactions include recombination (3-5) of the hydroxyl or hydrogen radical [15, 19, 21].

$$2\,OH^{\bullet} \rightarrow H_2O_2 \qquad (3)$$

$$2\,H^{\bullet} \rightarrow H_2 \qquad (4)$$

$$H^{\bullet} + OH^{\bullet} \rightarrow H_2O \qquad (5)$$

The high reactivity means that there are many more possible radical reactions. However, the concentration of radical is generally low, also due to the reactivity, which means that the reaction rate of these reactions are, as a result, often slow too, instead favoring the degradation reaction with higher reactant concentration.

3.2 Degradation of organic material

The high reduction potential of the hydroxyl radical drives the degradation of pollutants by oxidizing them. Given enough time, and and sufficient amount of hydroxyl radicals, all organic matter can be degraded fully into inorganic material, also called mineralization (6).

$$OH^{\bullet} + \text{organic material} \rightarrow CO_2 + H_2O + \text{inorganic material} \tag{6}$$

The hydroxyl radical can oxidize organic material in three ways; addition to double bonds and aromatic compounds, (7) including C=C, C=N, S=O, but excluding C=O. The reaction rate is fast, close to diffusion controlled. Hydrogen abstraction (8) from C-H, N-H, S-H or O-H. The reaction rate depends on the bond disassociation energy. The last is electron transfer reactions (9), which generally only occur when the other types are kinetically disfavored [13, 22, 23].

$$OH^{\bullet} + C{=}C \rightarrow OH{-}C{-}C^{\bullet} \tag{7}$$

$$OH^{\bullet} + R{-}H \rightarrow R^{\bullet} + H_2O \tag{8}$$

$$OH^{\bullet} + R{-}H \rightarrow [R{-}H]^{+\bullet} + OH^{-} \tag{9}$$

3.3 Degradation pathway of BAM

The degradation pathway of BAM has not been well studied. Madsen et al. [24] studied it using electrochemical oxidation. However, the degradation was only studied before ring cleavage. The proposed pathway is shown in **Figure 3**. The degradation starts with a substitution of a hydrogen with a hydroxy group in the para position, followed by the substitution of the two chloro groups with hydroxy groups as well. The next step results in ring cleavage.

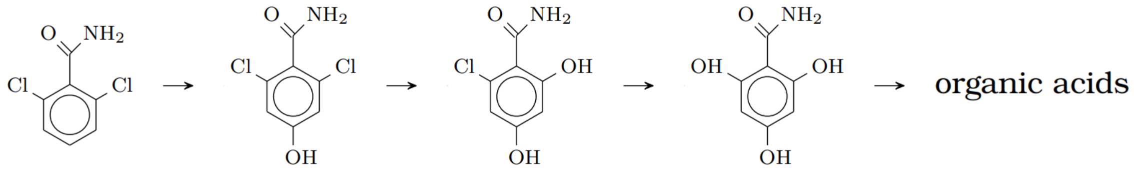

Figure 3: Proposed degradation pathway of BAM [24].

3.4 Process factors

3.4.1 Water composition

The groundwater matrix differs based on location, with different level of ionic species. Some of these ionic species can affect the degradation process due either absorption of the VUV radiation or reaction with the hydroxyl radical. Bicarbonate, chloride, nitrate and natural organic matter (NOM) can all scavenge hydroxyl radicals. Natural organic matter can scavenge hydroxyl radicals as shown in (6). Both Zhu et al. [25] and Yang et al. [26] tested this, and both showed a slower degradation of the target pollutants, with increased NOM. Bicarbonate can scavenge hydroxyl radical as shown in (10). The effect of bicarbonate is well studied, with severeal studies showing decreased degradation rate, with increased bicarbonate concentration [15, 16, 20, 27]. Nitrate can act as a hydroxyl radical scavenger (11)[15, 26] or absorb the VUV radiation (12)[14]. The latter can be a concern due to the nitrite generation, because of the difference in thresholds; 0.10 $\mathrm{mg\,L^{-1}}$ for nitrite versus 50 $\mathrm{mg\,L^{-1}}$ for nitrate [9].

$$\mathrm{HCO_3^- + OH^\bullet \rightarrow H_2O + CO_3^{\bullet -}} \tag{10}$$

$$\mathrm{NO_3^- + OH^\bullet \rightarrow NO_3^\bullet + OH^-} \tag{11}$$

$$\mathrm{NO_3^- + hv(185\ nm) \rightarrow NO_2^- + \frac{1}{2} O_2} \tag{12}$$

Chloride can also scavenge hydroxyl radicals, as shown in the reaction system (13-14), however this scavenging is mostly relevant at lower pH as can be seen by (14) [15, 16, 20, 25]. Duca [16] investigated the balance between hydroxyl and chloride radicals in 1.5 mM chloride concentration. At pH 5.2 only 13.2% percent of the hydroxyl radicals was converted into chloride radicals, and this decreased to 4.1% at pH 5.6. This not only means that chloride can inhibit degradation of the target compound in lower pH, but the chloride radical can also possibly react with the target compound and produce chlorinated byproducts. However, studies by Furatian [20] and Duca [16], have only shown low or no formation of chlorinated byproducts.

$$\mathrm{Cl^- + OH^\bullet \rightleftharpoons HOCl^{\bullet -}} \tag{13}$$

$$\mathrm{HOCl^{\bullet -} + H^+ \rightleftharpoons Cl^\bullet + H_2O} \tag{14}$$

Sulphate can increase the degradation rate, due to photon scavenging of VUV radiation leading the sulphate radicals (15). Sulphate radicals can also oxidize organic matter, as previously mentioned, but can also react with water to form hydroxyl radicals (16).

$$\mathrm{SO_4^{2-} + hv(185\ nm) \rightarrow SO_4^{-\bullet} + e_{aq}^-} \qquad \Phi = 0.64 \tag{15}$$

$$\mathrm{SO_4^{-\bullet} + H_2O \rightarrow HSO_4^- + OH^\bullet} \tag{16}$$

The generation of sulphate radicals have been shown to increase the degradation rate [16, 20, 26], due to the higher quantum yield for the photoreaction.

However, sulphate only weakly absorbs the radiation as can be seen by its molar absorption coefficient, shown in **Table 2**.
In addition to nitrate and sulphate, other matrix components can also scavenge the VUV photons. As can be seen in **Table 2**, nitrate and chloride most strongly absorb the radiation. This can inhibit the degradation, as less radiation absorbed by water results in lower formation of hydroxyl radicals. Non volatile organic matter (NVOC) can also absorb the radiation, here the nordic reservoir humic acid standard has been used as reference [16]. The high molar absorption coefficient for chloride suggest high inhibition in degradation, however this photoreaction results in formation of chloride radicals. As already explained chloride radicals can possibly aid in degradation, but not necessarily. Furatian [20] showed varied results, some organic compounds degraded faster with chloride present, some slower. Additionally, the chloride radicals can also form hydroxyl radical by (13-14). This means, that the inhibition of degradation is smaller, than what the photon scavenging potential of chloride suggests [16, 20].

Table 2: Water matrix components and their molar absorption coefficient [16].

Compound	ϵ (M^{-1} cm^{-1})
K^+	841
SO_4^{2-}	148
Ca^{2+}	109
HCO_3^-	269
NO_3^-	5568
Cl^-	2791
NVOC	1137

3.4.2 Flowrate, solution pH

Besides the effect from the water matrix, other variables capable of influencing the degradation. Both flowrate and solution pH can have an effect on the process. Flowrate has been tested by both Imoberdorf et al. [27] and Yang et al. [26]. Imoberdorf et al. [27] found an increase in degradation rate with increased flowrate, to a point, while Yang et al. [26] found an increasing flowrate resulted in worse degradation. However, these studies used two different setups. Imoberdorf et al. [27] used a recirculation setup, where the increased flow improved the mixing, to increase the degradation rate. Yang et al. [26] instead used a single pass setup, where the increased flowrate meant a shorter residence time, and less of the pollutants degraded.
Solution pH was studied in the range 5-9 by Yang et al. [26], where its impact was studied on five different pesticides: alachlor, aldicarb, clhoroneb, methiocarb and atrazine. The pH was found to have an effect of the degradation rate of these pesticides, however, it did not affect all of them similarly. Aldicarb showed fasted degradation with pH 7 and above, and methiocarb also showed greater degradation at high pH. However, the other three pesticides showed a

decrease in degradation rate, with increased pH. This suggests, that while pH does affect the rate of degradation, changing pH in water polluted with multiple pesticides is not useful, at least without testing the pH dependence for every pesticide. Changing pH would also impact the simplicity of the system, and as drinking water must be within pH 7-8.5 [9], the pH changes would either have to be very slight, or the pH would need to be readjusted after treatment, further complicating the system.

4. Reactor Modeling

Modeling a VUV reactor requires 3 things: a model for the emitted radiation, explaining photon absorption, a kinetic model, describing the kinetics for the desired reactions and reactor model, for the reactor mass balance. Both the radiation and reactor mass balance depend on the reactor, and for this study an annular-flow tubular reactor was used. A quick overview of the three models and their inputs and outputs are shown in **Figure 4**.

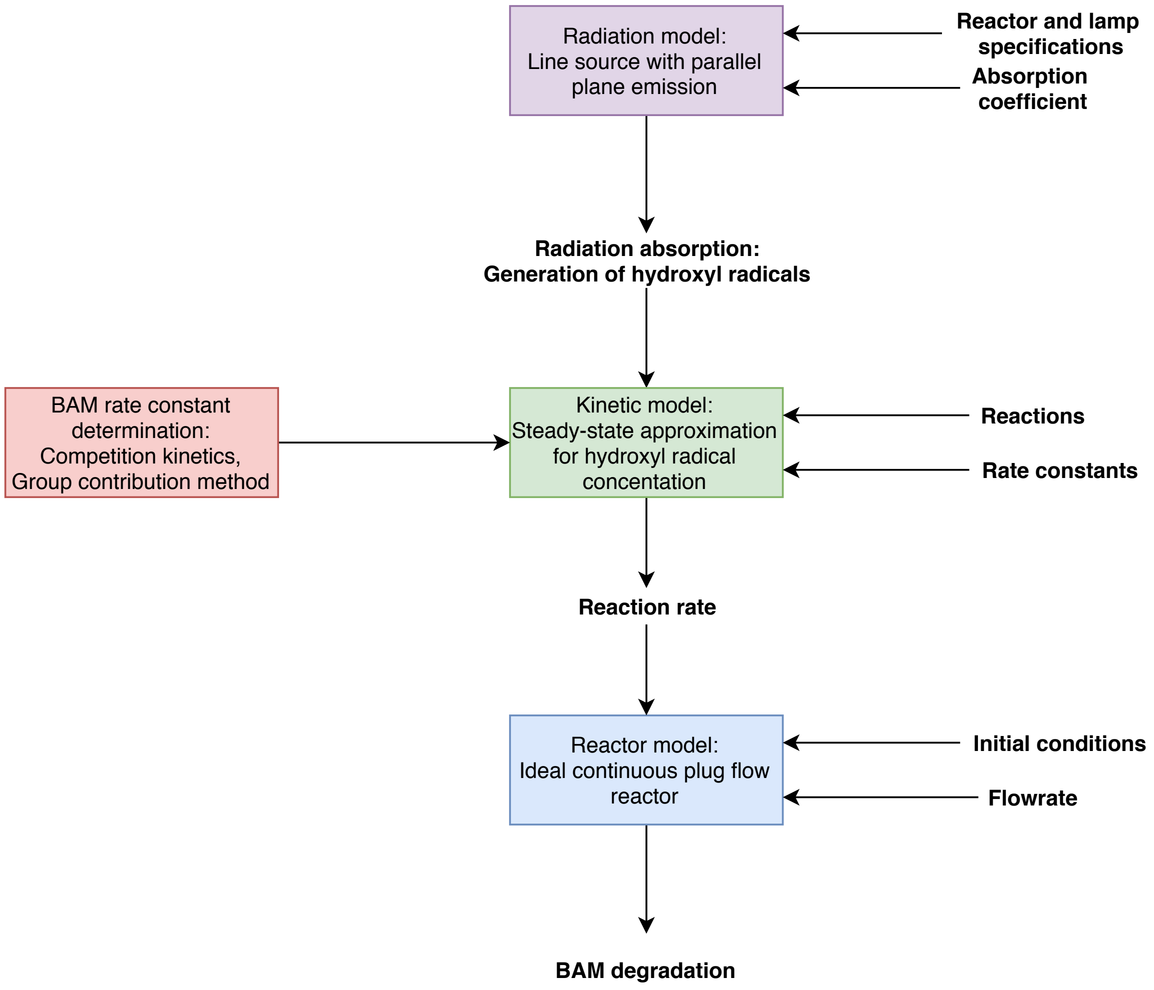

Figure 4: Overview of the used models required for modeling the degradation of BAM.

4.1 Radiation model

The radiation model is used for determining photon absorption, which is the source of hydroxyl radicals. Radiation emission models are split into two subgroups, line source and extense source models. Line source models uses the assumption that the lamp has no volume, while the extense source models, model the lamp as a cylinder with a volume. While extense source models are more realistic, they are also complex and require more computational power. Line source models can be further split into 3 groups, depending on how the emission in handled, either as a parallel plane emission, where the radiation is only emitting in the radial direction, as a diffuse emission, or as a spherical emission [28, 29] However, as most of the radiation is absorbed close to the quartz sleeve, the simple line source model with parallel plane emission (LSPP) is sufficient, as it has been shown to be just as effective in this area [19, 30], as more advanced models. The fluence rate distribution following the LSPP model, can be described as seen in (17) [19, 29–31].

$$I(r) = \frac{P_{UV}}{2\pi r L} \cdot 10^{-A(r-R_q)} \qquad r \geq R_q \tag{17}$$

Here A is the absorption coefficient of the absorbing species (m^{-1}), calculated as in (18), L is the length of the lamp (m), R_q is the quartz sleeve radius, P_{UV} is the radiation flux of the lamp at 185 nm (W), and r is the coordinate in the radial direction. This model assumes, (i) the radiation is only emitted in the radial direction, (ii) that no reflection or refraction occur and the air/quartz, quartz/water and water/reactor wall interfaces, (iii) that the model and lamp are the same length [28].

$$A = \sum \epsilon_i C_i \tag{18}$$

With the fluence rate distribution the local volumetric rate of photon absorption (LVRPA) can be found as shown in (19), where α_i is the napieran absorption coefficient of the absorbing species calculated using (20), and $x_{\lambda,i}$ is the fraction of photons absorbed by the species calculated using (22).

$$\mathrm{LVRPA}_i(\mathrm{r}) = \alpha I(r) x_{\lambda,i} \tag{19}$$

$$\alpha = A ln(10) = \sum \epsilon_i C_i ln(10) \tag{20}$$

By using the average integral over the radius, we can get the average volumetric rate of photon absorption (VRPA) for the reactor (21) [32]. Here R_r is the radius of the reactor (m). The unit for the VRPA is unit energy, per unit time and volume, and used in the form einstein L^{-1} s^{-1}.

$$\mathrm{VRPA}_i = \frac{1}{R_r} \int_{R_q}^{R_r} \mathrm{LVRPA}_i(\mathrm{r})\, dr \tag{21}$$

4.1.1 Photon scavenging

As explained in **Section 3.4**, the water matrix components can scavenge photons by absorbing the 185 nm radiation. The photon distribution was calculated by (22) [16, 19].

$$x_{\lambda,i} = \frac{\epsilon_i C_i}{\sum \epsilon_i C_i} \tag{22}$$

4.2 Reaction kinetics

The rate constant of BAM is needed to fully explain the kinetic system. Two methods was used for determining it, an experimental and a theoretical one. With the $OH^{\bullet}$ rate constant for BAM, the kinetic system can be derived.

4.2.1 Competition Kinetics

As hydroxyl radicals have so high reactivity, normal methods for determining rate constants for their reactions are ineffective. Direct methods of determining the rate constant can be difficult, if neither the reactants or products can be observed, as the decay rate of hydroxyl radicals cannot be measured accurately [33, 34]. Competition kinetics instead measures the relative rate constant to an easier observable reactant, such as a dye. In this study the dye, 4-nitrosodimethylaniline (RNO) was used (23), to determine the rate constant for (24) [33, 34].

$$\mathrm{OH^{\bullet} + RNO \rightarrow products} \qquad k_{RNO} = 1.25 \cdot 10^{10} \mathrm{M^{-1}\,s^{-1}} \tag{23}$$

$$\mathrm{OH^{\bullet} + BAM \rightarrow products} \tag{24}$$

In the competition between these two reactions equation the following two rate equations can be obtained (25-26). Now by dividing (25) with (26) we can derive (27) [35–37].

$$-\frac{dC_{\mathrm{OH^{\bullet}}}}{dt} = k_{RNO} C_{RNO} C_{\mathrm{OH^{\bullet}}} + k_{BAM} C_{BAM} C_{\mathrm{OH^{\bullet}}} \tag{25}$$

$$-\frac{dC_{RNO}}{dt} = k_{RNO} C_{RNO} C_{\mathrm{OH^{\bullet}}} \tag{26}$$

$$\frac{dC_{\mathrm{OH^{\bullet}}}/dt}{dC_{RNO}/dt} = 1 + \frac{k_{BAM} C_{BAM,0}}{k_{RNO} C_{RNO,0}} \tag{27}$$

Equation (27) is generally used for estimation hydroxyl rate constant, by equating $dC_{\mathrm{OH^{\bullet}}}/dt$ to the transient concentration change of a dye in absence of competition and equating dC_{RNO}/dt to the transient concentration change of the dye in the presence of competition. Kwon et al.[34] showed a similar model works in a continuous flow system (28), using the loss rate, or apparent rate constant, of dye in absence of competition S_0 and in presence of competition, S, together with the entry concentrations. This is found by assuming pseudo-first-order kinetics, using (29). By plotting S_0/S against $C_{BAM,0}/C_{RNO,0}$, the ratio between the rate constants can be found by the slope [34].

$$\frac{S_0}{S} = 1 + \frac{k_{BAM}C_{BAM,0}}{k_{RNO}C_{RNO,0}} \tag{28}$$

$$ln(C/C_0) = -kt \tag{29}$$

4.2.2 Rate constant prediction using GCM

The group contribution method (GCM) for determination of hydroxyl radical rate constansts, is based on the hypothesis that the rate constant for a given compound, depends on the sum of the rate of all elementary reactions with OH$^{\bullet}$. Minekata et al. [38] developed a procedure using this method to predict hydroxyl radical rate constants. The rate constants can be estimated with the activation energy, E_a, by using the Arrhenius equation (30), and for each reaction mechanism there a base activation energy and a contribution due to neighboring functional groups, $E_a^{R_i}$, from both the α and β position.

$$k = Ae^{-E_a/RT} \tag{30}$$

The method considers the rate constant for each reaction mechanism and the overall rate constant as the sum of these. As shown in **Section 3.2** OH$^{\bullet}$ degrades organic compounds in three ways. The GCM considers four reaction mechanisms, (i) hydrogen abstraction, (ii) OH$^{\bullet}$ addition to alkenes (iii) OH$^{\bullet}$addition to aromatic compounds and, (iv) OH$^{\bullet}$ interactions with sulphur, nitrogen or phosphorous containing compounds. The overall rate constant is the sum of rate constant for each of the four mechanisms (31).

$$k_{overall} = k_{abs} + k_{add-alkene} + k_{add-aromatic} + k_{int} \tag{31}$$

The rate of hydrogen atom abstraction depends on whether the bond is a primary, secondary or tertiary C-H bond. The partial rate constant for each C-H bond is split into a base rate constant based on (30) and part from functional groups shown in (32). The total rate constant due to hydrogen abstraction is then the sum of all the partial rate constants (33), where k_{R_4}, represents the rate constant for all functional groups.

$$X_{R_i} = e^{E^{R_i}_{a,abs}/RT} \tag{32}$$

$$k_{abs} = 3\sum k^0_{prim}X_{R_1} + 2\sum k^0_{sec}X_{R_1}X_{R_2} + \sum k^0_{tert}X_{R_1}X_{R_3}X_{R_3} + k_{R_4} \tag{33}$$

For double bond addition the base rate constant depends on the double bond structure, in general there are six main structures, >C=C<, H>C=C<, H_2C=C<, H>C=C<H (cis), H>C=C<H(trans), and H_2C=C<H. The group contribution is calculated similarly, and the total rate constant for addition to alkenes is the sum of all partial rate constants (34), where the h is either 1 or 2 depending

on which side $OH^{\bullet}$ add to, left or right respectively. Y_{R_l} is the group contribution factor, where l is the number of function groups, and g is either 1 or 2 depending on whether the addition is asymmetrical or not, respectively.

$$k_{add-alkene} = \sum g k^{0}_{(structure)-h} Y_{R_l} \tag{34}$$

Aromatic addition depends on both the structure of the aromatic compound, the position of functional groups, and the positions available for addition. Addition to the ipso position is neglected due to significant steric effect. The total rate constant for aromatic addition is shown in (35), where n is the number of availabe positions to add. Name refers to the aromatic structure, benzene, furan etc., i refers to the positions of the functional groups, and j refers to the positions for addition. Z_{R_m} is the functional group factor, where m is the number of functional groups.

$$k_{add-aromatic} = \sum n k^{0}_{(i-name)-j} Z_{R_m} \tag{35}$$

4.2.3 Kinetic system

The kinetic system in radical oxidation processes are very complex, consisting of many different radical reactions. However, the combination of a low concentration of the radical, and a low rate constant, many of these reactions can be neglected, greatly simplifying the kinetic system without changing the result. This study will neglect the effect of radical side reactions for these reasons, and to simplify the degradation model. The degradation model will instead include the effect of both the hydroxyl radical and photon scavenger identified in **Section 3.4**. Beyond the inorganic scavengers, NVOC will also be included. To simulate the organic carbon found in the groundwater, the nordic reservoir humic acid will be used, which [16] have previously studied, and identified both its absorption of 185 nm radiation, and its rate constant when reacting with $OH^{\bullet}$. The kinetic system and the rate constants are shown in **Table 3**.

Table 3: The kinetic scheme used for simulating groundwater conditions.

no.	Reaction	Constant	Ref
1	$H_2O + hv(185\text{ nm}) \rightarrow OH^{\bullet} + H^{\bullet}$	$\Phi_1 = 0.33\,\text{mol einstein}^{-1}$	[14]
2	$H_2O + hv(185\text{ nm}) \rightarrow OH^{\bullet} + H^{+} + e^{-}_{aq}$	$\Phi_2 = 0.045\,\text{mol einstein}^{-1}$	[14]
3	$SO_4^{2-} + hv(185\text{ nm}) \rightarrow SO_4^{\bullet-} \rightarrow OH^{\bullet}$	$\Phi_3 = 0.64$	[20]
4	$BAM + OH^{\bullet} \rightarrow \cdots \rightarrow$ inorganic material	-	-
5	$MCPA + OH^{\bullet} \rightarrow \cdots \rightarrow$ inorganic material	$k_6 = 4.55 \cdot 10^{9} M^{-1} s^{-1}$	[39]
6	$HCO_3^{-} + OH^{\bullet} \rightarrow H_2O + CO_3^{-\bullet}$	$k_4 = 8.5 \cdot 10^{8} M^{-1} s^{-1}$	[33]
7	$Cl^{-} + OH^{\bullet} \rightarrow HOCl^{\bullet-}$	$k_5 = 4.3 \cdot 10^{9} M^{-1} s^{-1}$	[33]
8	$HOCl^{\bullet-} \rightarrow Cl^{-} + OH^{\bullet}$	$k_5 = 6.1 \cdot 10^{9} M^{-1} s^{-1}$	[33]
9	$NO_3^{-} + OH^{\bullet} \rightarrow NO_3^{\bullet} + OH^{-}$	$k_6 =< 1 \cdot 10^{5} M^{-1} s^{-1}$	[33]
10	$NVOC + OH^{\bullet} \rightarrow \cdots \rightarrow$ inorganic material	$k_7 = 3.7 \cdot 10^{4} L\,mg^{-1} s^{-1}$	[16]

To simplify the reaction kinetics, the following assumptions were made: (i) that only the reactions shown in **Table 3** occur, and that no radical side reactions occur between hydroxyl radicals and, other hydroxyl radicals, hydrogen radicals, solvated electrons, or products of these. (ii) that the steady-state approximation (SSA) is applicable for hydroxyl radicals and the $OH^\bullet$ concentration is constant. (iii) potential radiation absorption of BAM and MCPA is neglected. The reaction system can now be defined by (36-37). The steady-state approximation can now be applied, which assumes no accumulation of hydroxyl radicals due to its high reactivity (38-39), where $R_{S,i}$ refers to the reaction rate of scavenger reactions (reactions 6-10). As the concentration of hydroxyl radicals is assumed to be constant, (39) will be evaluated using entry conditions [28, 32]. Looking further into (36) and (39) it can be seen, that in the absence of any competing reactions, i.e. in demineralised water, the rate of BAM degradation does not depend on the rate constant, but rather its concentration and the generation of hydroxyl radicals.

$$R_i = k_i C_i C_{\mathrm{OH}^\bullet} \tag{36}$$

$$R_{\mathrm{OH}^\bullet} = \mathrm{VRPA}_{\mathrm{H_2O}} \cdot \Phi_1 + \mathrm{VRPA}_{\mathrm{H_2O}} \cdot \Phi_2 - \sum R_i \tag{37}$$

$$R_{\mathrm{OH}^\bullet} = \mathrm{VRPA}_{\mathrm{H_2O}} \cdot \Phi_1 + \mathrm{VRPA}_{\mathrm{H_2O}} \cdot \Phi_2 - \sum R_i \cong 0 \tag{38}$$

$$C_{\mathrm{OH}^\bullet} = \frac{\mathrm{VRPA}_{\mathrm{H_2O}} \cdot \Phi_1 + \mathrm{VRPA}_{\mathrm{H_2O}} \cdot \Phi_2 + \mathrm{VRPA}_{\mathrm{SO_4}^{2-}} \cdot \Phi_3}{C_{BAM} k_{BAM} + C_{MCPA,0} k_{MCPA} + \sum C_{S,i} k_{S,i}} \tag{39}$$

4.3 Reactor model

The mass balance in the system is modeled using an ideal continuous plug flow reactor model (PFR). The concentration change in this model depends on the reactor volume, due to the relation between residence time and reactor volume in this type of reactor. The balance is shown in (40), where it relates the change in molar flowrate, dF_i, and change in reactor volume dV, with the reaction rate for the reaction happening inside the reactor, R_i.

$$\frac{dF_i}{dV} = R_i \tag{40}$$

5. Research Objective

The objective of this study is to construct a suitable kinetic model for the degradation of BAM using VUV, and assess the possibilities for cleaning pesticide polluted groundwater using VUV at a waterwork.

How can the VUV process be scaled for cleaning groundwater of BAM?

Investigation of this problem includes both theoretical and experimental work. Determination of the rate constant for the degradation reaction of BAM will be found experimentally. With the kinetic system explained, the degradation can be modeled with increasing complexity. Experimental validation of the degradation model was planned, however the necessary resources were unavailable. A summary of the modeling and experimental work can be seen in **Figure 5**.

1. To explain the kinetic scheme, competition kinetics will be used to find the rate constant for the degradation reaction for BAM. This will be done by comparing the difference in degradation of the dye 4-nitrosodimethylaniline with increasing BAM concentration in the solution, and then finding the rate constant for BAM relative to the dye. Additionally, a group contribution method will also be used to determine it theoretically.
2. The degradation will then be modeled, firstly in 1 $\mathrm{mg\,L^{-1}}$ scale, with increasing water complexity, starting with demineralized water and adding different matrix components to emulate drinking water.
3. The degradation will then be modeled in the scale found in groundwater, to assess the sizing of reactor needed for cleaning groundwater of BAM to below the threshold.

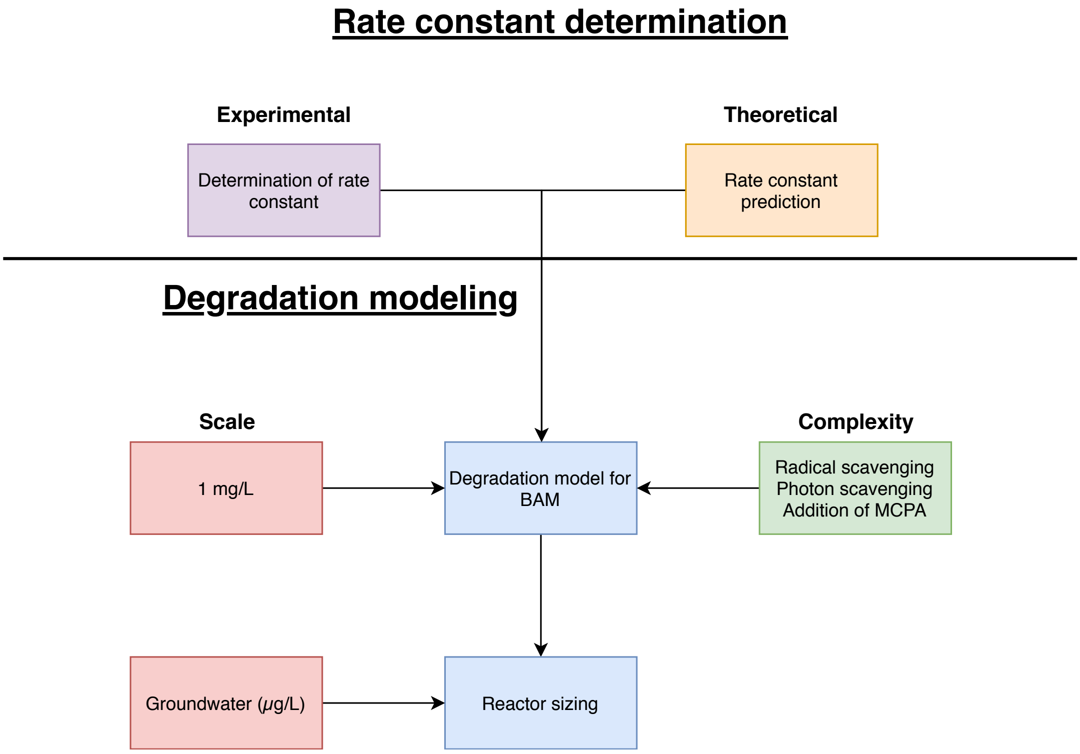

Figure 5: Flowchart of the performed experimental and modeling work.

6. Materials and Methods

For determining the reaction rate of BAM using competition kinetics, ≥95% 4-nitrosodimethylaniline dye from Fluka was used, together with ≥98% 2,6-dichlorobenzamide from Sigma-Aldrich.

UV/Vis Spectrophotometry

Ultraviolet-visible light spectrometry was used for determining the concentration of the RNO dye. Uv/Vis is useful for measuring the concentration of dyes, a sample is irradiated with light of a specific wavelength in the UV/Vis region and the absorbance of the light in measured. The absorbance is proportional to the concentration, as can be seen in the Beer-Lambert equation (41), where A is absorbance, ϵ is the molar absorbance coefficient, and b is path length [40].

$$A = \epsilon bc \tag{41}$$

6.1 Experimental setup

The experimental setup consisted of the VUV reactor and lamp, pump and recirculation tank. A process flow diagram can be seen in **Figure 6**.

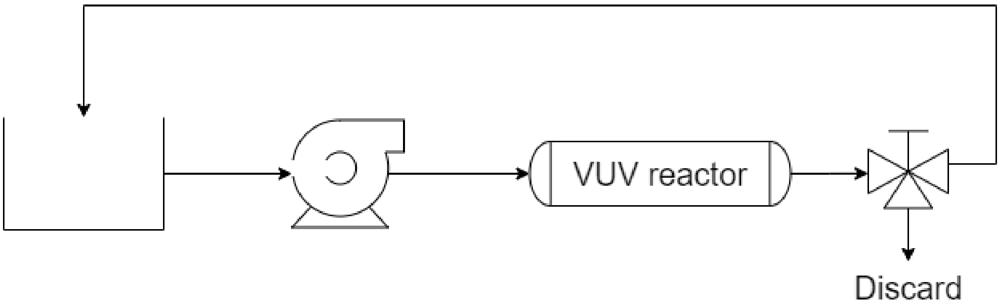

Figure 6: Process flow diagram of the experimental setup.

Lamp

The lamp is a LP Hg lamp with emissions at 254 and 185 nm, with a 19 mm diameter and an arc length of 1050 mm. The 185 nm emission intensity is 25% of the 254 nm emission, with a radiation flux at 14 W compared to 56 W, with a power input of 200 W.

Reactor

The reactor is an annular-flow tubular reactor in stainless steel with internal diameter of 53 mm and a length of 1097 mm. The lamp is positioned in the middle of the reactor with a high purity quartz sleeve around it, which has a diameter of 28 mm. This gives the reactor a total volume of 1.74 L. The reactor has an opening at the side for a UV sensor which measures the 254 nm radiation, with a maximum irradiance measured around 360 $\mathrm{W\,m^{-2}}$

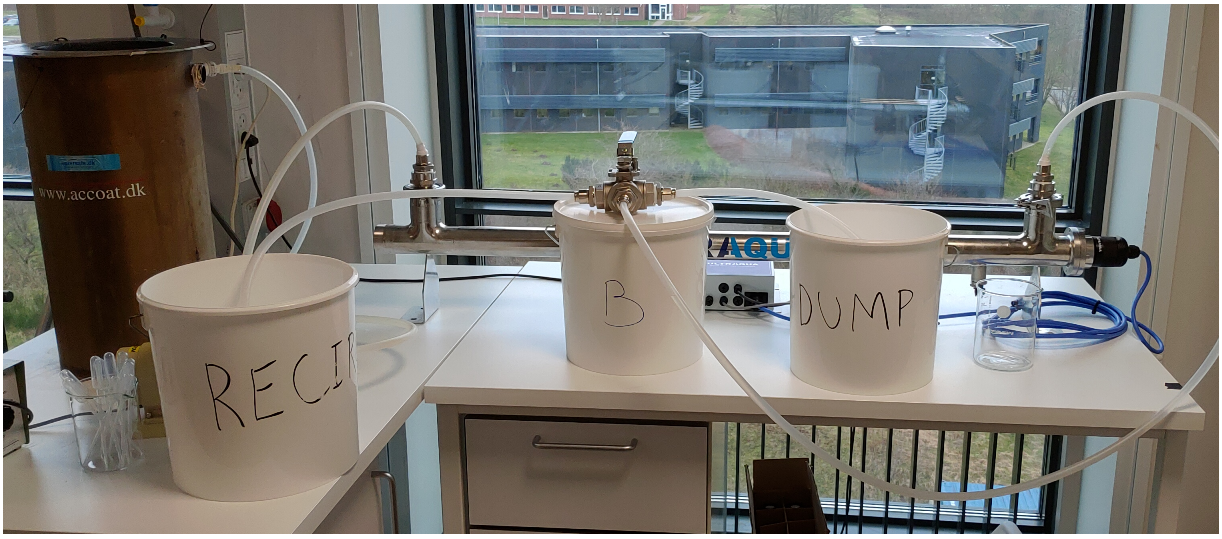

Figure 7: The experimental setup.

6.2 Experimental procedure

The experimental part was performed using the setup shown in **Figure 6** and **Figure 7**. The tank was charged with 10 L of dye, or dye and BAM solution. A dye concentration of 2 $\mathrm{mg\,L^{-1}}$ was used, with BAM concentration corresponding to 1, 2, 5 and 10 times the dye concentration on mass basis, the equivalent on mole basis is shown in **Table 4**. The lamp was turned on and when an approximate of 360 $\mathrm{W\,m^{-2}}$ was achieved, the solution was pumped through the reactor once, with a flowrate of 2.25 $\mathrm{L\,min^{-1}}$. The dye concentration was measured both at the beginning, and after the single pass, using UV/Vis spectrophotometry. Each experiment was performed in duplicates.

Table 4: Different solutions used for determining the rate constant of BAM using competition kinetics.

RNO ($\mathrm{mg\,L^{-1}}$)	RNO(μM)	BAM ($\mathrm{mg\,L^{-1}}$)	BAM (μM)	$C_{BAM,0}$ / $C_{RNO,0}$
2	13.72	0	0	0
2	13.72	2	10.52	0.79
2	13.72	4	21.05	1.58
2	13.72	10	52.62	3.95
2	13.72	20	105.25	7.90

6.3 Modeling procedure

The modeling was performed using MATLAB for determining the VRPA for water and sulphate using (17-21), where the absorption coefficient used for water was 1.80 cm^{-1}. The generation of hydroxyl radicals was then calculated using the quantum yields for each possible hydrolysis (Reaction 1-3 in **Table 3**. From there, the differential equation shown in (40) was used, where the rate expression for BAM was input in the form shown in (36). In the rate expression, the steady-state concentration of $\text{OH}^{\bullet}$ was used (39). This gives the final expression, shown in (42), with the relation between molar flowrate F, and concentration C, shown in (43), where Q is the volumetric flowrate. To keep it consistent with the experimental work, the same volumetric flowrate was used, 2.25 $\text{L}\,\text{min}^{-1}$. This was evaluated using the entry condition (44). In case of MCPA addition, (42) was evaluated for both BAM and MCPA. The differential equation was solved using the numerical differiential equation solver in the Chemical Reaction Engineering module in COMSOL Multiphysics.

$$\frac{dF_i}{dV} = k_{BAM} C_{BAM} \cdot \frac{\text{VRPA}_{\text{H}_2\text{O}} \cdot \Phi_1 + \text{VRPA}_{\text{H}_2\text{O}} \cdot \Phi_2 + \text{VRPA}_{\text{SO}_4^{2-}} \cdot \Phi_3}{C_{BAM,0} k_{BAM} + C_{MCPA,0} k_{MCPA} + \sum C_{S,i,0} k_{S,i}} \tag{42}$$

$$F_i = QC_i \tag{43}$$

$$F_{BAM,0} = QC_{BAM,0} \tag{44}$$

7. Results

7.1 Rate constant determination

To fully explain the reaction kinetics of the degradation of BAM, its associated $OH^\bullet$ rate constant is needed. Two methods were used to determine this rate constant, competition kinetics, an experimental method, and group contribution method, a theoretical method, as explained in **Section 4.2**. Both of these rate constants will then be used in evaluating the degradation of BAM in groundwater.

7.1.1 Competition Kinetics

Degradation of RNO with increasing BAM concentration was done to assess the rate constant for the degradation reaction for BAM. The apparent rate constant for degradation of RNO dye was estimated with increasing BAM concentration to study competition between the two reactions. The different ending concentrations for the RNO dye are shown in **Table 5**. These concentrations were used to estimate the apparent rate constants. **Figure 8** shows the relation between S_0/S, and increasing BAM concentration. As the figure and table shows, the increasing BAM concentration influences the degradation of the dye, decreasing the apparent rate constant to about to about 40% with a starting concentration 7.9 times higher. The slope is found to be 0.187, together with a good linear fit at R^2 at 0.972. The rate constant can now be found with the slope using (28) and the rate constant of RNO, $1.25 \cdot 10^{10}$ $M^{-1}\,s^{-1}$, resulting in a rate constant of $2.34 \pm 0.37 \cdot 10^9$ $M^{-1}\,s^{-1}$, where the uncertainty represents the 95% confidence interval. Looking at **Figure 8** the last point seem a bit too low, however removing this point only increases the rate constant slightly, increasing it to $2.81 \cdot 10^9 M^{-1}\,s^{-1}$.

Table 5: Dye concentration after a single pass and estimated apparent rate constants.

$C_{BAM,0}/C_{RNO,0}$	C_{end} ($mg\,L^{-1}$)	k'(s^{-1})
0	0.218	0.0482
0.79	0.318	0.0400
1.58	0.382	0.0360
3.95	0.618	0.0255
7.90	0.791	0.0202

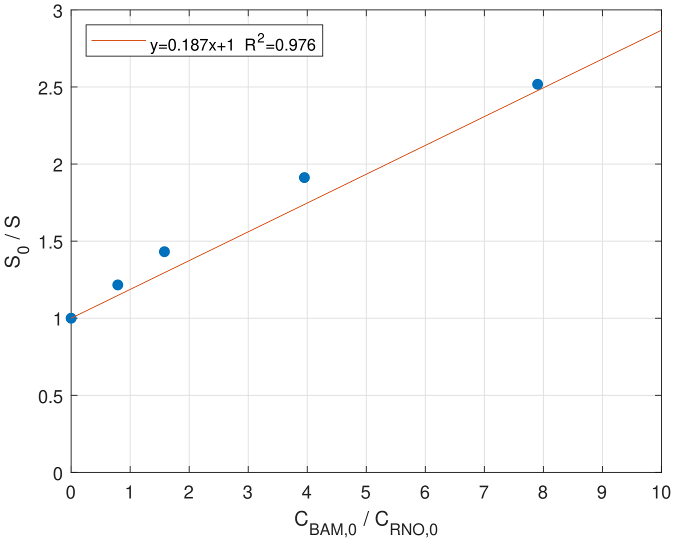

Figure 8: Competition kinetics between RNO and BAM.

7.1.2 Predicted rate constant

The hydroxyl radical rate constant for the degradation of BAM was also predicted using GCM. As BAM contains no aliphatic C-H or C=C bonds, the only contributing factors to the rate constant is the rate for aromatic addition, and the interaction rate with the amide group. The hydroxyl radical rate constant for BAM can now be predicted by (45-46), which results in a predicted rate constant of $4.88 \cdot 10^9 \mathrm{M}^{-1}\,\mathrm{s}^{-1}$. This is slightly higher, than what was experimentally determined, and provides strong evidence that the OH$^\bullet$ rate constant for BAM lies in this range.

$$k_{BAM} = (2k^0_{(1,2,3-benz)-4,6} + k^0_{(1,2,3-benz)-5}) Z_{-Cl} Z_{-Cl} Z_{-\mathrm{CONH_2}} + k_{-\mathrm{CONH_2}} \tag{45}$$

$$\begin{aligned} k_{BAM} = {} & (2 \cdot 2.15 \cdot 10^9 \mathrm{M}^{-1}\,\mathrm{s}^{-1} + 1.64 \cdot 10^9 \mathrm{M}^{-1}\,\mathrm{s}^{-1}) \cdot 0.9781^2 \cdot 0.8422 \\ & + 9.98 \cdot 10^7 \mathrm{M}^{-1}\,\mathrm{s}^{-1} = 4.88 \cdot 10^9 \mathrm{M}^{-1}\,\mathrm{s}^{-1} \end{aligned} \tag{46}$$

7.2 Water base

To simulate drinking water in Denmark, the water composition from a local waterwork, Vognsbøl Vandværk, was used. This water composition was used in analyzing the degradation of BAM in $1\,\mathrm{mg\,l^{-1}}$ and groundwater scale. The composition is shown in **Table 6**, and the water has a solution pH of 8.0. Of the radical scavengers, bicarbonate and chloride are both in fairly high concentration, and when comparing with the rate constant in **Table 3**, NVOC as well. The photon scavenging effect from matrix components are also seen in **Table 6**, where the percentage of photons absorbed by each component is determined using (22). By far the biggest photon scavenger is chloride, with bicarbonate

Table 6: Water matrix of groundwater from Vognsbøl Vandværk and photon scavenging from each component [41].

Compound	Concentration		% of 185 photons
	$(\mathrm{mg\,L^{-1}})$	(M)	
K^+	2.1	$5.4 \cdot 10^{-5}$	0.80
SO_4^{2-}	17	$1.8 \cdot 10^{-4}$	0.46
Ca^{2+}	50	$1.2 \cdot 10^{-3}$	2.39
HCO_3^-	149	$2.4 \cdot 10^{-3}$	11.56
NO_3^-	0.50	$8.1 \cdot 10^{-6}$	0.79
Cl^-	37	$1.0 \cdot 10^{-3}$	51.28
NVOC	0.62	$1.0 \cdot 10^{-2*}$	1.03
H_2O	-	55.49	31.69

*:Calculated using $M_C = 12.01\ \mathrm{g\,mol^{-1}}$.

scavenging second most, scavenging only 11.56% compared to the 51.28% of chloride. In groundwater scale, water from Esbjerg was analyzed and compared with water from two other waterworks in Denmark, Staurbyskov Vandværk in Middelfart and Hvidovre Vandværk in Hvidovre. Their compositions, together with absorption of the radiation is shown in **Table 7**. Both of these

Table 7: Water matrix of groundwater from Staurbyskov and Hvidovre Vandværk and photon scavenging from each component [42, 43].

Compound	Concentration		% of 185 photons
	$(\mathrm{mg\,L^{-1}})$	(M)	
Middelfart			
K^+	2.3	$5.9 \cdot 10^{-5}$	0.68
SO_4^{2-}	87	$9.1 \cdot 10^{-4}$	1.85
Ca^{2+}	120	$3.0 \cdot 10^{-3}$	4.50
HCO_3^-	313	$5.1 \cdot 10^{-3}$	19.03
NO_3^-	4.2	$6.8 \cdot 10^{-5}$	5.20
Cl^-	39	$1.1 \cdot 10^{-3}$	42.34
NVOC	1.2	$1.0 \cdot 10^{-4*}$	1.57
H_2O	-	55.49	24.83
Hvidovre			
K^+	5	$1.3 \cdot 10^{-4}$	0.82
SO_4^{2-}	86	$9.0 \cdot 10^{-4}$	1.01
Ca^{2+}	116	$2.9 \cdot 10^{-3}$	2.40
HCO_3^-	380	$6.2 \cdot 10^{-3}$	12.76
NO_3^-	1.8	$2.9 \cdot 10^{-5}$	1.23
Cl^-	111	$3.1 \cdot 10^{-3}$	66.55
NVOC	2.1	$1.8 \cdot 10^{-4*}$	1.52
H_2O	-	55.49	13.71

*:Calculated using $M_C = 12.01\ \mathrm{g\,mol^{-1}}$.

types of water leads to a higher percentage of photon scavenging when compared to **Table 6**, down to 24.83% and 13.71% absorption of 185 nm radiation from water, for Middelfart and Hvidovre water respectively. While this is a large difference in percentage of photons absorbed by water, this does not directly explain the difference in $OH^{\bullet}$ generation. While a smaller fraction of photons absorbed is absorbed by water in Middelfart and Hvidovre water, there is also a larger absorption of the radiation, due to the more absorbant species present, specifically the increase in bicarbonate, and for Hvidovre, chloride as well. This means that the decrease in $OH^{\bullet}$ is lower than what **Table 6** and **7** suggests. The difference $OH^{\bullet}$ generation is shown in **Table 8**, where it can be seen that the generation of $OH^{\bullet}$ only decreases by 13% and 51%, for Middelfart and Hvidovre water respectively, compared to the 21% and 57%, suggested by **Table 6** and **7**.

Table 8: Difference in $OH^{\bullet}$ generation between the three types of groundwater.

	$OH^{\bullet}$ gen. ($M\,s^{-1}$)	Compared to Esbjerg water
Esbjerg	$9.8 \cdot 10^{-7}$	1.00
Middelfart	$8.5 \cdot 10^{-7}$	0.87
Hvidovre	$4.8 \cdot 10^{-7}$	0.49

7.3 BAM degradation in 1 $mg\,L^{-1}$ scale

Each scavenging effect was analyzed by itself to evaluate the effect on the degradation in 1 $mg\,L^{-1}$ scale in Esbjerg water. Three effects were considered, hydroxyl radical scavenging, photon scavenging and inhibition due to addition of MCPA. All degradation was modeled using the same flow rate that was used for the experimental determination of the rate constant, 2.25 $L\,min^{-1}$.

7.3.1 Hydroxyl radical scavenging

In drinking water it is clear that the concentration of $OH^{\bullet}$ scavengers inhibit the degradation of BAM. Of the identified scavengers in **Section 3.4**, nitrate and chloride has been excluded. Nitrate is not included, both due to the low rate constant and its low concentration found in drinking water from Esbjerg as shown in **Table 6**, which together means that nitrate only have a very limited capability for inhibiting the degradation of BAM through $OH^{\bullet}$ scavenging. Chloride, on the other hand, has both a high concentration and rate constant. Chloride scavenges hydroxyl radical by the reaction system shown in (13-14). As the modeled water has a pH of 8, (14) has a very low reaction rate, and almost no $Cl^{\bullet}$ is formed. As the rate constant of the reverse scavenging reaction is higher (**Table 3**) and with chloride competing for hydroxyl radicals, any scavenged $OH^{\bullet}$, is immediately formed again, leading to no inhibition of BAM degradation. This was confirmed by the model. **Figure 9a** shows the degradation of BAM in absence and in the presence of $OH^{\bullet}$ scavengers, using the experimentally found rate constant. Bicarbonate and NVOC inhibit the degradation similarly, and together they visibly inhibit the degradation of BAM. The reactor length needed for 90% degradation increases from approximately 0.11 m in demineralized water to 0.28 and 0.31 m in the presence of bicarbonate and NVOC respectively, and to 0.49 m in the presence of both scavengers. The larger rate constant for BAM, found theoretically using GCM, naturally results in faster BAM degradation, as shown in **Figure 9b**. The inhibtion of BAM degradation from the $OH^{\bullet}$ scavengers is greatly reduced. The reactor volume needed for 90% degradation is now only increased to 0.19 and 0.20, for bicarbonate and NVOC and 0.28 m for all scavengers.

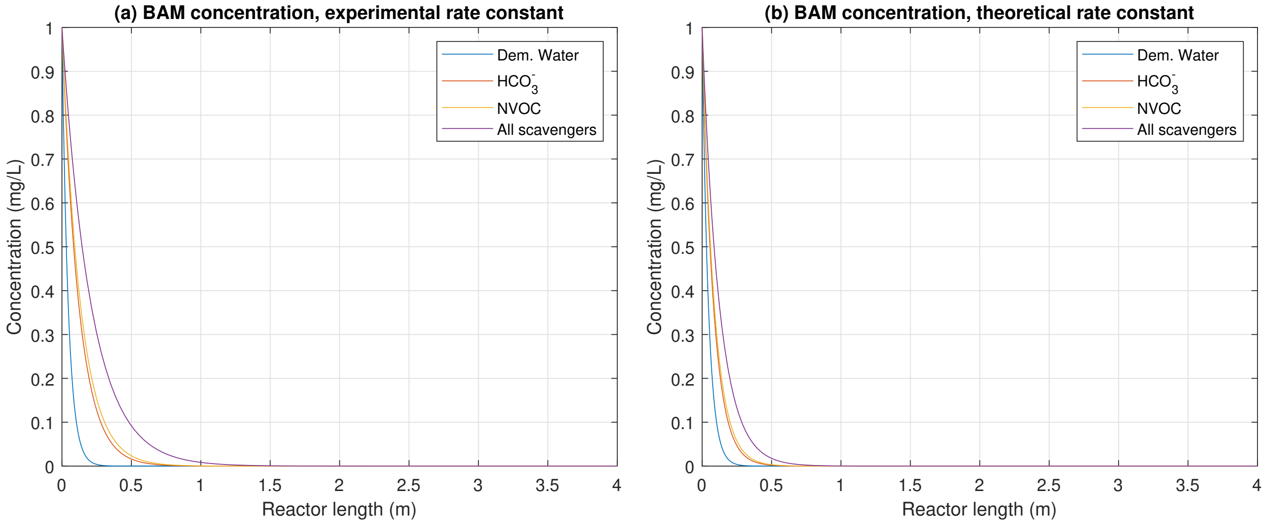

Figure 9: Degradation of BAM in 1 $mg\,L^{-1}$ scale with and without $OH^{\bullet}$ scavengers, using (a) the experimental rate constant and (b) the theoretical rate constant.

7.3.2 Photon scavenging

Photon scavenging decreases the percentage of photons absorbed by water down to only 32% (**Table 6**). While photons absorbed by sulphate in theory increases the degradation rate, the concentration found in the groundwater is not high enough to absorb a sizeable amount of the radiation, when in the presence of stronger absorbing species such as bicarbonate and chloride. The effect of sulphate has been added to the model, by assuming all the formed sulphate radicals are converted into hydroxyl radicals, however this only accounts for 2.42% of the generated hydroxyl radicals, with the remaining forming due to water photolysis. While the amount of photons scavenged by chloride is high, the effect on the degradation have been shown to not be quite as high. The chloride radicals formed due to radiation absorption from chloride, can form hydroxyl radicals as seen in (14). This means that the effect of photon scavenging from chloride is smaller than what appears in **Table 6**. As this effect has not been fully researched, it will be neglected [20]. Photon scavenging only affects the generation of hydroxyl radicals, and modeling photon scavenging alone, without any competing reactions yields the same result independent on the rate constant used, for the same reason the rate constant does not affect the degradation in demineralized water. The effect of both photon and hydroxyl radical scavenging can be seen in **Figure 10a**, which shows the modeled degradation using the experimentally found rate constant. Photon scavenging by itself has a smaller effect on the degradation, requiring 0.29 m for 90% degradation against the 0.46 m from radical scavengers. Including both types of scavenging leads to a much slower degradation, needing 1.35 m for 90% degradation. With the theoretical rate constant, **Figure 10b**, the effect of radical scavengers is lessened, and very similar to the effect of photon scavenging. The reactor length needed for degradation of 90% is very close, with 0.28 m needed with radical scavenging, and 0.29 m for photon scavenging. This greatly reduces the reactor length needed for 90% degradation with both scavengers, down to 0.80 m.

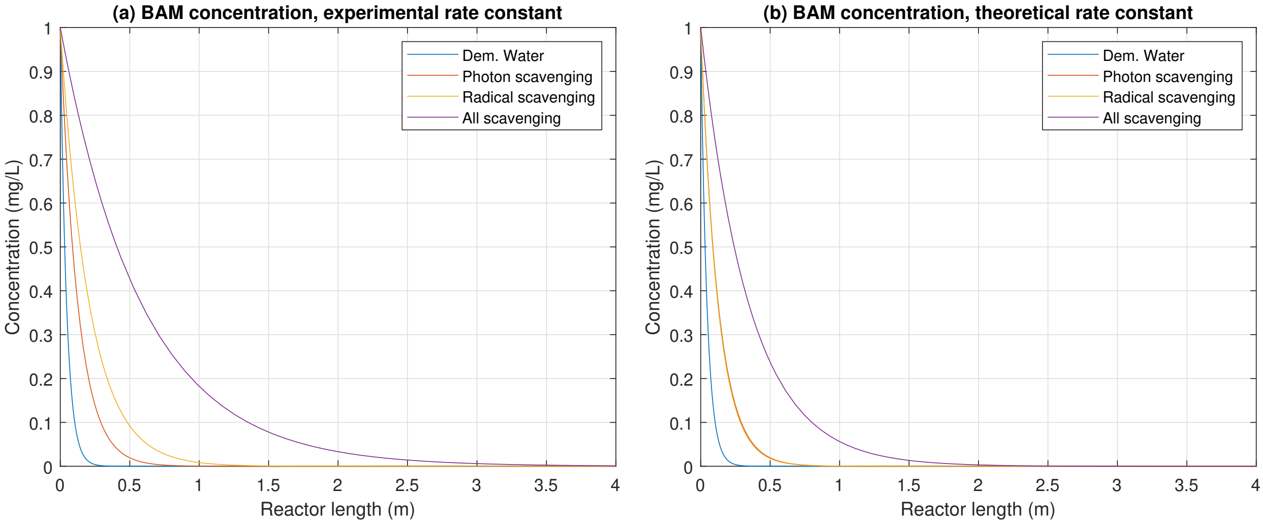

Figure 10: Degradation of BAM in 1 $\mathrm{mg\,L^{-1}}$ scale with photon and $OH^{\bullet}$ scavengers, using (a) the experimental rate constant and (b) the theoretical rate constant.

7.3.3 Multiple pesticide pollution

As groundwater is not only polluted with one pesticide, MCPA was added to the model to see how it affects the reactor length needed to degrade multiple pesticides. The addition of other pesticides, have the same effect as radical scavenging on the degradation of BAM, however, in contrast to other radical scavengers, MCPA also needs to be degraded. In a review by Wols et al. [39], the average reported rate constant for MCPA in the litterature was found to be $k = 4.55 \cdot 10^9 \mathrm{M}^{-1}\,\mathrm{s}^{-1}$. The two rate constants indicate the difference in degradation, when using the experimental rate constant for BAM, MCPA will clearly be degraded first, while using the theoretical rate constant for BAM, the two pesticides will degrade at a more similar rate. This is shown **Figure 11**, where (a) shows the degradation with the experimental rate constant and (b) shows it with the theoretical rate constant, in demineralized water. With the experimental BAM rate constant, the reactor length needed for at least 90% degradation of both pesticides is 0.29 m compared to the 0.21 m with the theoretical BAM rate constant. The addition of MCPA increased the needed reactor volume from 0.11 m for BAM only, to similar levels needed when adding one of the two hydroxyl radical scavengers.

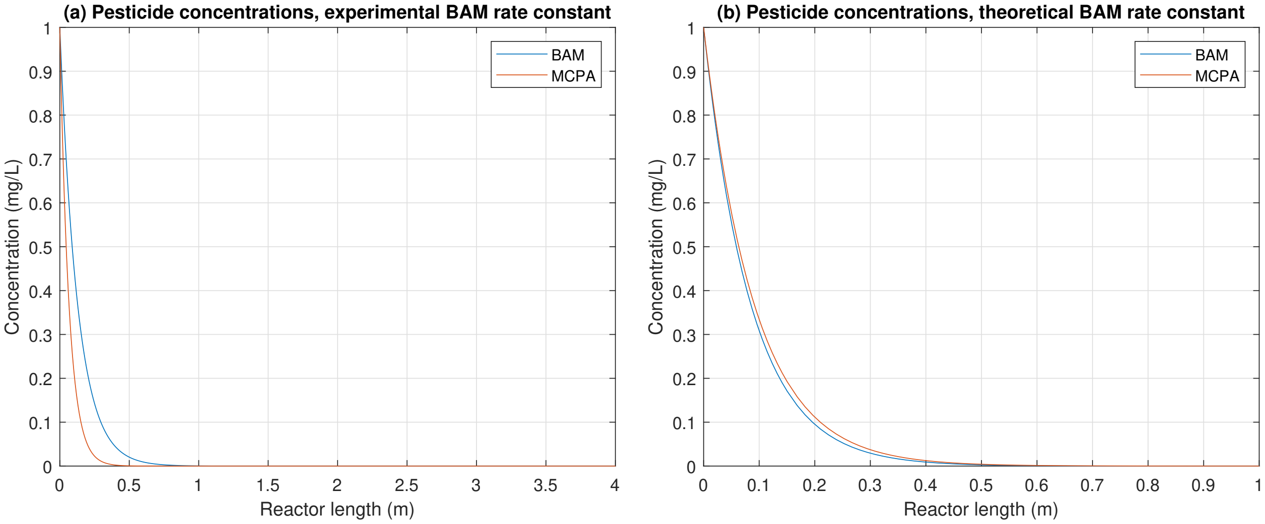

Figure 11: Degradation of BAM and MCPA in 1 $\mathrm{mg\,L^{-1}}$ scale in demineralized water using (a) the experimental BAM rate constant and (b) the theoretical BAM rate constant.

7.3.4 All factors

To properly model the degradation of BAM in groundwater, all the influencing factors are needed. **Figure 12** shows the size of each effect on the degradation of BAM. Using the experimental rate constant (**Figure 12a**), the biggest effect is radical scavenging, while the addition of MCPA and photon scavenging show similar inhibition of BAM degradation. The sum of all three result in much slower BAM degradation, which now requires a reactor length of 1.77 m for 90% degradation. In **Figure 12b**, using the theoretical rate constant, the effects are much smaller, with photon scavenging and radical scavenging now having similar inhibition on BAM degradation. This means much lower reactor volume is needed for 90% degradation, now only needing 1.06 m. The difference in degradation between BAM and MCPA with all effects, is not that critical. When using the experimental BAM rate constant, the BAM degradation is the important, as it is slower, while using the theoretical BAM rate constant the degradation between the two are very similar. The conclusion using the experimental BAM rate constant is unchanged, but using the theoretical BAM rate constant, the reactor length needed for at least 90% for all pesticides is slightly increased, to 1.18 m.

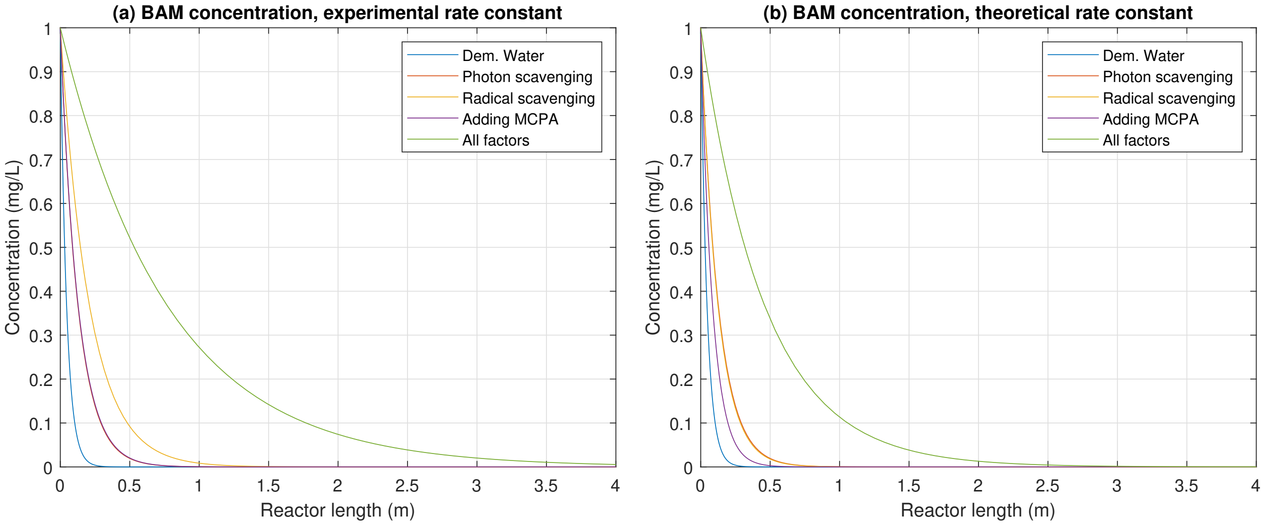

Figure 12: Degradation of BAM in 1 $\mathrm{mg\,L^{-1}}$ scale with all factors, using (a) the experimental rate constant and (b) the theoretical rate constant.

7.4 BAM degradation in groundwater scale

The degradation of BAM was modeled in the scale found in groundwater, to evaluate the use of the reactor for cleaning groundwater of pesticides. The initial BAM concentration was changed in the interval 0.2-0.5 $\mu g\,L^{-1}$, using Esbjerg water in **Table 6**. All scavenging effects are included, and the degradation was tested both with BAM only, but also in the presence of different MCPA concentrations. **Figure 13** shows the BAM degradation without addition of MCPA, where the x-axis now show the number of passes through the reactor, and the red line shows the threshold. This is done to evaluate the amount of the modeled reactor is needed to degrade BAM below the threshold. As seen in **Figure 13a**, to degrade just up to 0.5 $\mu g\,L^{-1}$ one pass through the reactor is enough, needing the equivalent of 0.29 to 0.65 reactors to degrade BAM below the threshold, when using the experimental rate constant. However, when using the higher theoretical rate constant (**Figure 13b**), only half of the reactor is needed, ranging from 0.15 to 0.33 reactor passes. Thus, these results show that only one pass through the reactor is ever needed to degrade BAM below the threshold, if the groundwater is only polluted with BAM.

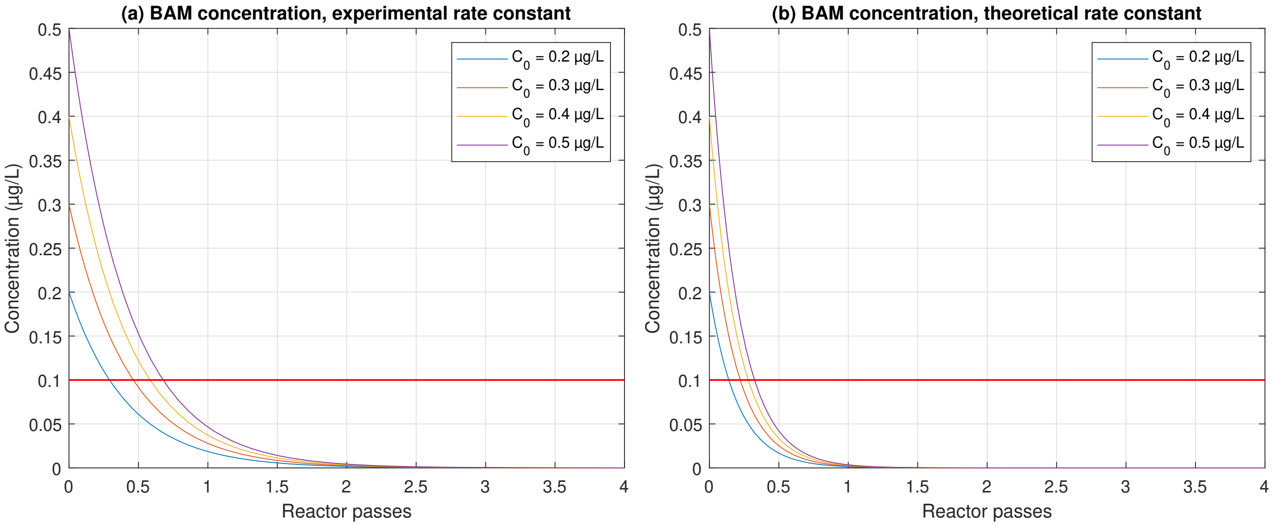

Figure 13: Degradation of BAM in groundwater scale with photon and $OH^{\bullet}$ scavengers, using (a) the experimental rate constant and (b) the theoretical rate constant.

7.4.1 Effect of multiple pesticides

The inhibitory effect of other pesticides present, was simulated with increasing initial MCPA concentration. The reaction rate for BAM when adding other pollutants is affected by the decrease in steady state $OH^•$ concentration (39), and this depends on two things, the concentration of the pollutant and its rate constant. In the absence of rate constants for the other prominent pesticides found in Danish groundwater, this was instead simulated by increasing the initial MCPA concentration to levels much higher than what is found in groundwater. This is shown in **Figure 14**, where it can be seen that a very high pesticide concentration is needed to inhibit the degradation. The change in degradation rate is nearly absent with MCPA concentration of 0-10 $\mu g\,L^{-1}$, and only slightly noticeable at 100 $\mu g\,L^{-1}$. In fact, 1 $mg\,L^{-1}$ is needed to see a noteworthy change, increasing the needed reactor passes to 1.05 using the experimental rate constant, and to 0.50 when using the theoretical. This would suggest that BAM degradation is not majorly inhibited by other pesticides found in the groundwater, unless their rate constant is significantly larger than that of MCPA. This also means that, any pesticide which has a rate constant similar to the experimental rate constant for BAM or higher, will also be degraded. If their rate constant is significantly smaller, the scavenger reactions would be more favoured, but otherwise, the VUV reactor is capable of degrading all other pesticides present, without needing to majorly increase the reactor size, or amount of reactors.

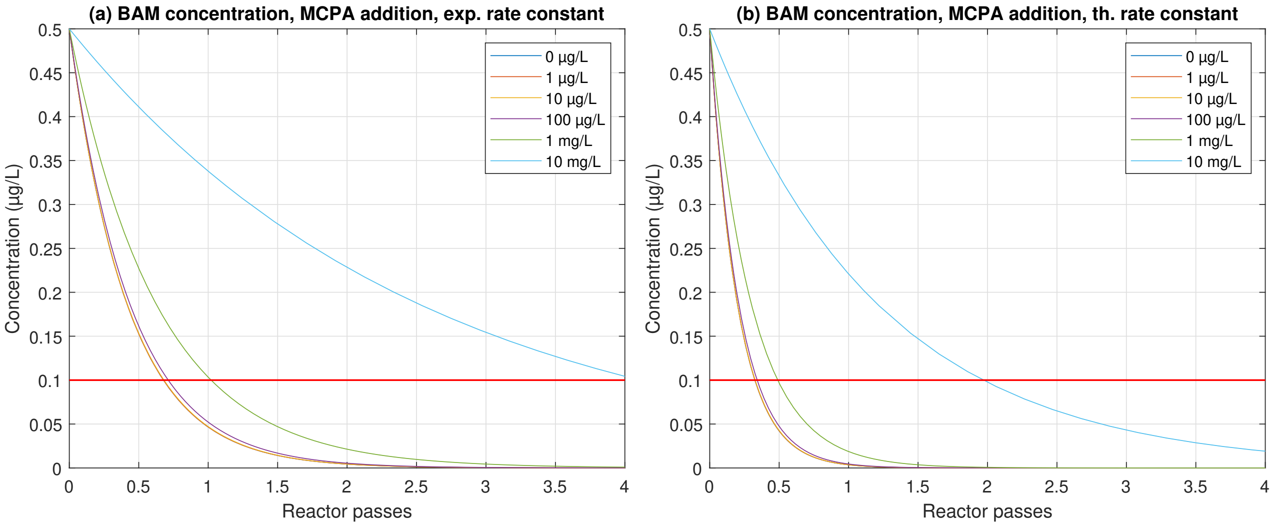

Figure 14: Degradation of BAM in groundwater scale with photon and $OH^•$ scavengers and increasing MCPA concentration, using (a) the experimental rate constant and (b) the theoretical rate constant.

7.4.2 Effect of composition

The degradation model in groundwater scale was performed on two other types of drinking water, from other parts of Denmark, as described in **Table 7**. Unsurprisingly, both groundwater from Middelfart and Hvidovre have slower BAM degradation than water from Esbjerg, as both of these types of groundwater have higher amount of photon and radical scavengers. The degradation of these three water compositions are shown in **Figure 15**. The increased concentration of scavengers, means that the equivalent amount of reactors needed for degrading BAM below the threshold, when using the experimental rate constant, rises from 0.65 in Esbjerg water to 1.53 for Middelfart water. Water from Hvidovre is by far the worst, needing slightly more than 4 reactor passes before degrading BAM below the threshold. Using the theoretical rate constant (**Figure 15b**) yields slightly better results, however, Hvidovre water still requires considerable more reactor passes, increasing to 1.90 reactor passes, compared to the lower amount needed for Middelfart and Esbjerg water at 0.71 and 0.33 respectively. The capacity of the modeled system is much lower than the demand of a waterworks, with the modeled flow rate being only 2.25 $\mathrm{L\,min^{-1}}$, or 0.135 $\mathrm{m^3\,h^{-1}}$. As the main component of the degradation is treatment time, any increases to the flow rate, would only result in needing an equivalent amount of extra reactor passes for degradation below the threshold.

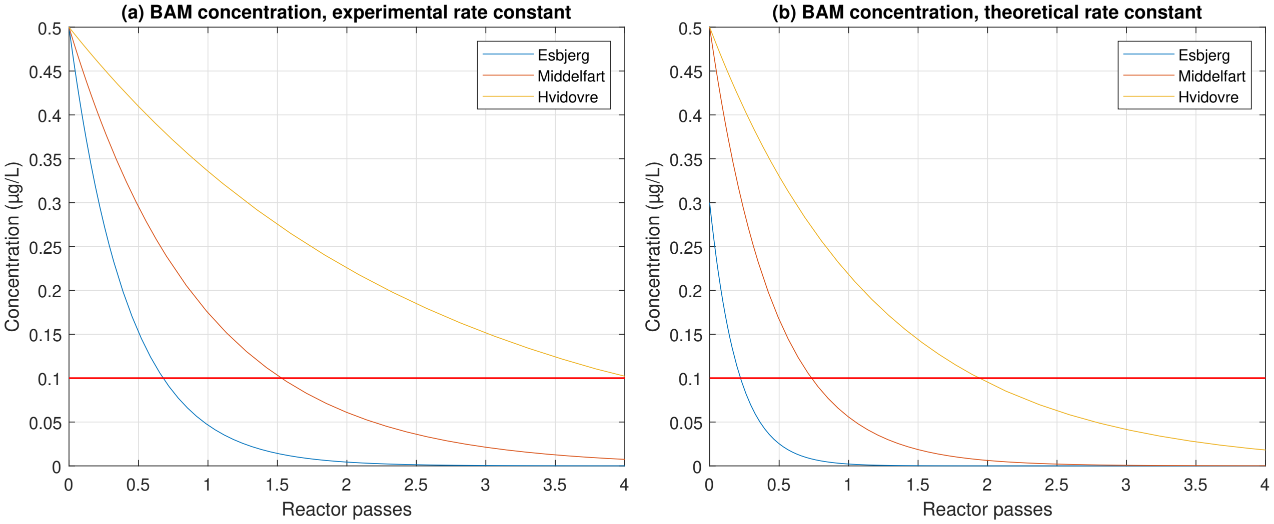

Figure 15: Degradation of BAM in groundwater scale with photon and $OH^{\bullet}$ scavengers and different water compositions, using (a) the experimental rate constant and (b) the theoretical rate constant.

7.5 Energy consumption

The energy consumption was considered, using the electrical energy-per-order, E_{EO}, which is the amount of electrical energy, in kilowatt-hours, needed to degrade the pollutant one order (90%), in 1 $\mathrm{m^3}$ of water [26, 44, 45]. In a photochemical continuous system this can be calculated by (47), where P is the electrical power used in kW, Q is the flowrate in $m^3 h^{-1}$, and C_0 and C_i are the initial and exit concentrations, respectively. The exit concentration refers to the concentration after one pass in the reactor.

$$E_{EO} = \frac{P}{Qlog(C_0/C_i)} \tag{47}$$

The E_{EO}, was calculated based on the data shown in **Figure 15**, and the results are shown in **Table 9**, neglecting pump energy usage. The values using the experimental rate constant are approx. twice as big as those using the theoretical rate constant, and the theoretical rate constant is also approx. twice than the experimental one. The values vary more when looking at the different water types, where the E_{EO} in Hvidovre water is approximately six times higher than the value in Esbjerg water, while Middelfart water resides in the middle. These values range from the lower middle end to the higher middle end based on a review by Miklos et al. [45], where some of the median values are shown in **Table 10**. The main competing technology, UV/H_2O_2, has an median E_{EO} of 0.75.

Table 9: The calculated E_{EO} values for each water type and rate constant, neglecting pump energy usage.

Water	Exp. k_{BAM}	Th. k_{BAM}
Esbjerg	1.46	0.69
Middelfart	3.28	1.56
Hvidovre	8.69	4.12

Table 10: Median E_{EO} values for different types of AOPs [45].

Technology	Median E_{EO}	Technology	Median E_{EO}
Ozonation	0.15	UV/H_2O_2	0.75
O_3/H_2O_2	0.2	Photo-Fenton	2.6
UV/chlorine	0.39	Plasma	3.3
UV/persulphate	0.67	Electrochemical	38.1
O_3/UV	0.70	UV/catalyst	335

However, the electrical energy-per-order is not constant for all types of applications. In groundwater applications the median E_{EO} for UV/H_2O_2 increases to 2.7. Thus, VUV degradation of BAM in groundwater from Esbjerg possibly has lower energy use than UV/H_2O_2, while eliminating the need for addition of H_2O_2. For Middelfart water, VUV only has higher energy efficiency if the pesticide has a rate constant similar to, or higher than, $4.88 \cdot 10^9 M^{-1} s^{-1}$, while for Hvidovre water VUV has lower energy efficiency. However, as can be seen in **Table 9** the E_{EO} heavily depend on the type of groundwater, so it is unclear how UV/H_2O_2 perform against VUV with the same type of groundwater. As the E_{EO} values presented for VUV here are without considering the energy usage of the pump, the true E_{EO} values for VUV degradation of BAM are higher.

8. Discussion

The objective of this study was to model the degradation of BAM using a VUV reactor, and assess the opportunities for using VUV in cleaning pesticide polluted groundwater, based on the results obtained. As only the degradation of BAM, and to a lesser extent MCPA, have been investigated, these were used as models for the other pesticide pollutants found in groundwater, however, further study on these is needed, most vitally their $OH^{\bullet}$ rate constants. As the majority of this study was modeling based, experimental results are needed to validate these results.

The $OH^{\bullet}$ rate constant for BAM, was determined using both an experimental and theoretical method. Both of these methods showed somewhat similar rate constants, $2.34\text{-}4.88 \cdot 10^{9}$ M^{-1} s^{-1}, giving strong indication that the rate constant is similar to, or in, this range. The experiment determined the rate constant, by observing how addition of BAM affected the apparent rate constant for the degradation of RNO dye. However, the apparent rate constant was estimated using only a single pass through the reactor, instead of longer monitoring, which is needed to precisely determine the apparent rate constant.

It is clear that scavengers, both radical and photon, greatly affect the degradation of BAM, and other pesticides. Four potential radical scavengers were identified based on literature review: bicarbonate, chloride, nitrate and NVOC. However, from the four, only two are viable in groundwater conditions, as nitrate are only found in low concentration, and the high pH inhibits the scavenging by chloride. Bicarbonate and NVOC showed to inhibit BAM degradation similarly in Esbjerg water, and as the ratio between their concentration is similar in Middelfart water this was the case there as well. In Hvidovre water the concentration of NVOC is proportionally higher, which leads to a larger proportional inhibition due to this component. For photon scavengers, chloride scavenges by far the most photons, followed by bicarbonate. The lower amount of photons absorbed by water leads to lower $OH^{\bullet}$ generation, inhibiting BAM degradation. Both NVOC and nitrate also have high potential for photon scavenging, but due to the lower concentration found in groundwater, they do not absorb nearly as much radiation as chloride and bicarbonate, even though the molar absorption coefficient for nitrate is twice as high than chloride, while the molar absorption coefficient for NVOC is four times higher than the molar absorption coefficient for bicarbonate.

Chloride was the main photon scavenger, and in lower pH, it would also be the main radical scavenger due to its high rate constant. However, the product of this scavenging, the chloride radical, can also affect the system. The chloride radical can contribute to the degradation, both by degrading some organic compounds, but also form hydroxyl radicals. The modeling performed in this study have neglected these effects, as they are not well understood. Thus, experimental results of BAM degradation could be faster than what is predicted in this study, due to this effect. While degradation by the chloride radical has only shown to form limited chlorinated byproducts, this still needs to be monitored.

This study mostly studied BAM polluted or BAM and MCPA polluted groundwater. While groundwater may be polluted by more than two pesticides, due to their low concentration they should not inhibit the degradation of the other pesticides, and as shown, $100\ \mu g\,L^{-1}$ of MCPA is needed to noticeably inhibit BAM degradation. Thus, multiple pesticide pollution should not be of concern, as the modeling shows the VUV reactor can degrade all without inhibition. However, if other pesticide pollutant have lower rate constants than the experimentally determined rate constant for BAM, this will lead to slower degradation, as scavenger reactions become more favoured.

Energy consumption is always an important factor, and this study have shown, that VUV can, depending on the type of groundwater, compete with the more established method using UV/H_2O_2. If this is confirmed experimentally, VUV would be a very cost effective solution for degrading pesticides, compared to UV/H_2O_2, eliminating addition of chemicals.

9. Conclusion

To investigate how a VUV reactor can be scaled for degrading BAM in groundwater, the degradation of BAM was kinetically modeled in an annular-flow tubular reactor. The rate constant for BAM was determined both experimentally, using the VUV reactor, and theoretically. The used VUV reactor had a reactor volume of 1.74 L, and used a low-pressure mercury lamp as source of VUV radiation, with a 185 nm emission.

The hydroxyl radical rate constant for BAM was determined experimentally using competition kinetics, where BAM was in competition with RNO dye, while a group contribution method was used for determining the rate constant theoretically. The two methods showed similar results, the experimental method yielded a rate constant of $2.34 \cdot 10^9\ \mathrm{M^{-1}\,s^{-1}}$, while the theoretical method predicted $4.88 \cdot 10^9\ \mathrm{M^{-1}\,s^{-1}}$. With both methods predicting similar results, this provides strong evidence that the rate constant is in the area of the two values.

The degradation of BAM was modeled in $1\ \mathrm{mg\,L^{-1}}$ scale in Esbjerg water. Two components contributed to hydroxyl radical scavenging, bicarbonate and NVOC, which acted similarly. Bicarbonate and chloride most strongly absorbed the radiation, and thus acted as photon scavengers, preventing $OH^{\bullet}$ generation. Comparing radical and photon scavenging, showed radical scavenging inhibited the BAM degradation more, when using the experimental rate constant, while they were near identical when using the theoretical.

In groundwater scale, the degradation model was studied, together with the effect of multiple pesticide pollution and composition. In Esbjerg water a single pass through the reactor was sufficient for degrading BAM, independent of the rate constant used. The initial BAM concentrations was varied between 0.2-0.5 $\mathrm{\mu g\,L^{-1}}$, and to degrade BAM below the threshold the equivalent of 0.29-0.65 reactors were needed with the experimental rate constant, compared to the 0.15-0.33 needed using the theoretical. MCPA was added to simulate pollution with multiple pesticides, and an addition of at least 100 $\mathrm{\mu g\,L^{-1}}$ was needed before a noticeable effect was seen on BAM degradation. As such, as long as other pesticides polluting the groundwater does not have a significantly lower rate constant than BAM, the VUV reactor can sufficiently manage the degradation of multiple pesticide pollutants. The water composition was varied using groundwater from Middelfart and Hvidovre. These both showed a higher concentration of scavengers, which heavily affected BAM degradation. The amount of equivalent reactors needed for degradation of below the threshold increased from 0.33-0.65 in Esbjerg water to 0.71-1.53 for Middelfart water and 1.90 to above 4 for Hvidovre water, depeding on the rate constant.

Lastly, to evaluate the energy consumption, the electrical energy-per-order was determined for each water type. In Esbjerg water 0.69-1.46 $\mathrm{kW\,h\,m^{-3}\,order^{-1}}$ was needed. The energy consumption increased in the two other water types, needing 1.56-3.28 in Middelfart water, while 4.12-8.69 was needed in Hvidovre water. While VUV in general is a promising technology for groundwater treatment due to its fast degradation of BAM, in Esbjerg water it seems especially promising with its low energy consumption as well.

10. Perspectives

This study has shown a potential for using VUV for degradation of BAM in groundwater. However, as this all depends on modeling work, experimental work is still needed to validate the results shown here. As BAM degradation was studied 1 $\mathrm{mg\,L^{-1}}$ scale, using a plug flow reactor model, a similar experimental setup is needed. This would involve pumping the feed through the reactor, taking a sample, before pumping through again, thus giving a dataset that would be comparable to what was modeled. However, due to the fast degradation predicted in this study, an increase in inital concentration might be neccessary.

As the effect chloride has on the system is not completely understood, this is an important thing to research to fully explain the system. This is especially important when considering higher chloride containing types of groundwater, such as the water found in Hvidovre. Although this would not compromise water quality, as the current model overpredicts scavenging from chloride, this could help scaling reactor size better for higher chloride containing groundwater.

In terms of capacity, different reactor sizes need to be further studied. While this study showed great degradation of BAM the low flowrate at 0.135 $\mathrm{m^3\,h^{-1}}$, does not provide the necessary capacity. Larger reactors need to be studied, to better increase the scale, and to provide the needed capacity. While increase in diameter of the reactor is not helpful, as the increased capacity would not be subject to VUV radiation, longer reactors, or multilamp reactors, could provide the higher capacity needed.

Lastly, this study focused on the degradation of BAM alone. However, when treating groundwater for pesticides, the degradation of the pollutants themselves are not enough, as no pesticide residue is allowed. Measuring the decrease in total organic carbon is vital in determining the potential of technology.

Bibliography

[1] Simone Etwil. Nye målinger afslører 75 pesticider i det danske grundvand. *Ingeniøren*, 2019. URL `https://ing.dk/artikel/nye-maalinger-afsloerer-75-pesticider-danske-grundvand-225611`.

[2] Søren Rask Petersen. Alarmerende ny opgørelse: Pesticider i fire ud af ti vandboringer. *Ingeniøren*, 2019. URL `https://ing.dk/artikel/alarmerende-ny-opgoerelse-pesticider-fire-ud-ti-vandboringer-225299`.

[3] HOFOR. Fund af stoffet DMS på vandværker i Dragør og Hvidovre, 2018. URL `https://www.hofor.dk/vandnyhed/fund-stoffet-dms-paa-vandvaerker-dragoer-hvidovre/`.

[4] Bente Villumsen. Videregående vandbehandling. Technical report, Naturstyrelsen, 2012.

[5] Townson. H. Public health impact of pesticides used in agriculture. *Transactions of The Royal Society of Tropical Medicine and Hygiene*, 86(3):350, 1992. doi: 10.1016/0035-9203(92)90345-D.

[6] GEUS. Vi påvirker grundvandet, 2019. URL `https://www.geus.dk/udforsk-geologien/laering-om-geologi/viden-om/viden-om-grundvand/vi-paavirker-grundvandet/`.

[7] Svar på S 4867 om fastsættelse af grænseværdier for pesticider i drikkevand, fra miljøministeren, 2004. URL `http://webarkiv.ft.dk/?/samling/20031/udvbilag/mpu/almdel_bilag1191.htm`.

[8] Lærke Thorling, Christian Nyrop Albers, Claus Ditlefsen, Vibeke Ernstsen, Birgitte Hansen, Anders R. Johnsen, and Troldborg Lars. Grundvandsovervågning Status og udvikling 1989-2017. Technical report, GEUS, 2019.

[9] Miljø- og Fødevareministeriet. Bekendtgørelse om vandkvalitet og tilsyn med vandforsyningsanlæg, 2019.

[10] Magnus Bredsdorff. 400.000 københavnere drikker vand med rester af nyopdaget stof, 2019. URL `https://ing.dk/artikel/400000-koebenhavnere-drikker-vand-med-rester-nyopdaget-stof-223828`.

[11] Mahdi Nikbakht Fini, Henrik Tækker Madsen, and Jens Muff. The effect of water matrix, feed concentration and recovery on the rejection of pesticides using NF/RO membranes in water treatment. *Separation and Purification Technology*, 215(September 2018):521–527, 2019. ISSN 18733794. doi: 10.1016/j.seppur.2019.01.047.

[12] Ole Hylling, M. Nikbakht Fini, Lea Ellegaard-Jensen, Jens Muff, Henrik Tækker Madsen, Jens Aamand, and Lars Hestbjerg Hansen. A novel hybrid concept for implementation in drinking water treatment targets micropollutant removal by combining membrane filtration with biodegradation. *Science of the Total Environment*, 694:133710, 2019. ISSN 18791026. doi: 10.1016/j.scitotenv.2019.133710.

[13] A. Gil, L.A. Galeano, and M.A. Vincente. *Applications of Advanced Oxidation Processes (AOPs) in Drinking Water Treatment*. Springer, 2018. ISBN 978-3319768816.

[14] Kristin Zoschke, Hilmar Börnick, and Eckhard Worch. Vacuum-UV radiation at 185nm in water treatment - A review. *Water Research*, 52:131–145, 2014. ISSN 00431354. doi: 10.1016/j.watres.2013.12.034.

[15] Tünde Alapi, Krisztina Schrantz, Eszter Arany, and Zsuzsanna Kozmér. Vacuum UV radiation-driven processes. *Water Intelligence Online*, 16:195–239, 2017. ISSN 1476-1777. doi: 10.2166/9781780407197{_}0195.

[16] Clara Duca. *Effect of water matrix on Vacuum UV process for the removal of organic micropollutants in surface water*. PhD thesis, University of Torino, 2015.

[17] Pengchao Xie, Siyang Yue, Jiaqi Ding, Ying Wan, Xuchun Li, Jun Ma, and Zongping Wang. Degradation of organic pollutants by Vacuum-Ultraviolet (VUV): Kinetic model and efficiency. *Water Research*, 133:69–78, 2018. ISSN 18792448. doi: 10.1016/j.watres.2018.01.019. URL `https://doi.org/10.1016/j.watres.2018.01.019`.

[18] Laith Furatian. Advanced Oxidation Radiation : Unlocking the Hidden Power of Low-Pressure Mercury Lamps. *UV Solutions*, 2019. URL `https://uvsolutionsmag.com/articles/2019/advanced-oxidation-radiation-unlocking-the-hidden-power-of-low-pressure-mercury-lamps/`.

[19] F. Crapulli, D. Santoro, M. R. Sasges, and A. K. Ray. Mechanistic modeling of vacuum UV advanced oxidation process in an annular photoreactor. *Water Research*, 64:209–225, 2014. ISSN 18792448. doi: 10.1016/j.watres.2014.06.048. URL `http://dx.doi.org/10.1016/j.watres.2014.06.048`.

[20] Laith Furatian. *The use of 185 nm radiation for drinking water treatment*. PhD thesis, University of British Columbia, 2017. URL `https://open.library.ubc.ca/cIRcle/collections/ubctheses/24/items/1.0348109`.

[21] Gustavo Imoberdorf and Madjid Mohseni. Modeling and experimental evaluation of vacuum-UV photoreactors for water treatment. *Chemical Engineering Science*, 66(6):1159–1167, 2011. ISSN 00092509. doi: 10.1016/j.ces.2010.12.020. URL `http://dx.doi.org/10.1016/j.ces.2010.12.020`.

[22] Stefan H. Bossmann, Esther Oliveros, Sabine Göb, Silvia Siegwart, Elizabeth P. Dahlen, Leon Payawan, Matthias Straub, Michael Wörner, and André M. Braun. New evidence against hydroxyl radicals as reactive intermediates in the thermal and photochemically enhanced fenton reactions. *Journal of Physical Chemistry A*, 102(28):5542–5550, 1998. ISSN 10895639. doi: 10.1021/jp980129j.

[23] C. Von Sonntag. Advanced oxidation processes: Mechanistic aspects. *Water Science and Technology*, 58(5):1015–1021, 2008. ISSN 02731223. doi: 10.2166/wst.2008.467.

[24] Henrik Tækker Madsen, Erik Gydesen Søgaard, and Jens Muff. Study of degradation intermediates formed during electrochemical oxidation of pesticide residue 2,6-dichlorobenzamide (BAM) in chloride medium at boron doped diamond (BDD) and platinum anodes. *Chemosphere*, 120: 756–763, 2015. ISSN 18791298. doi: 10.1016/j.chemosphere.2014.10.058.

[25] Shumin Zhu, Bingzhi Dong, Yangtao Wu, Lingjun Bu, and Shiqing Zhou. Degradation of carbamazepine by vacuum-UV oxidation process: Kinetics modeling and energy efficiency. *Journal of Hazardous Materials*, 368 (August 2018):178–185, 2019. ISSN 18733336. doi: 10.1016/j.jhazmat.2019.01.043. URL `https://doi.org/10.1016/j.jhazmat.2019.01.043`.

[26] Laxiang Yang, Mengkai Li, Wentao Li, Yuejie Jiang, and Zhimin Qiang. Bench- and pilot-scale studies on the removal of pesticides from water by VUV/UV process. *Chemical Engineering Journal*, 342(February):155–162, 2018. ISSN 13858947. doi: 10.1016/j.cej.2018.02.075. URL `https://doi.org/10.1016/j.cej.2018.02.075`.

[27] Gustavo Imoberdorf and Madjid Mohseni. Degradation of natural organic matter in surface water using vacuum-UV irradiation. *Journal of Hazardous Materials*, 186(1):240–246, 2011. ISSN 03043894. doi: 10.1016/j.jhazmat.2010.10.118. URL `http://dx.doi.org/10.1016/j.jhazmat.2010.10.118`.

[28] Thomas Coenen, Wim Van de Moortel, Filip Logist, Jan Luyten, Jan F.M. Van Impe, and Jan Degrève. Modeling and geometry optimization of photochemical reactors: Single- and multi-lamp reactors for UV–H2O2 AOP systems. *Chemical Engineering Science*, 96:174–189, 2013. doi: https://doi.org/10.1016/j.ces.2013.03.056.

[29] M Alfano and E Cassano. Radiation field modelling in photoreactors - I. Homogeneous media. *Chemical Engineering Science*, 41(1955):421–444, 1986.

[30] Dong Liu, Joel Ducoste, Shanshan Jin, and Karl Linden. Evaluation of alternative fluence rate distribution models. *Journal of Water Supply: Research and Technology - AQUA*, 53(6):391–408, 2004. ISSN 00037214. doi: 10.2166/aqua.2004.0031.

[31] José Plácido and Claudio Augusto Oller Nascimento. 2D-LSPP: An improved line source with parallel plane emission (LSPP) model for photon distribution in annular reactors. *Industrial and Engineering Chemistry Research*, 46(23):7587–7597, 2007. ISSN 08885885. doi: 10.1021/ie070078p.

[32] Maia Lescano, Cristina Zalazar, Alberto Cassano, and Rodolfo Brandi. Kinetic modeling of arsenic (III) oxidation in water employing the UV/H2O2 process. *Chemical Engineering Journal*, 211-212:360–368, 2012. ISSN 13858947. doi: 10.1016/j.cej.2012.09.075. URL `http://dx.doi.org/10.1016/j.cej.2012.09.075`.

[33] George V. Buxton, Clive L. Greenstock, W. Phillips Helman, and Alberta B. Ross. Critical Review of rate constants for reactions of hydrated electrons, hydrogen atoms and hydroxyl radicals (·OH/·O– in Aqueous Solution. *Journal of Physical and Chemical Reference Data*, 17(2):513–886, 1988. ISSN 15297845. doi: 10.1063/1.555805.

[34] Bum Gun Kwon, Seongyun Ryu, and Jeyong Yoon. Determination of hydroxyl radical rate constants in a continuous flow system using competition kinetics. *Journal of Industrial and Engineering Chemistry*, 15(6):809–812, 2009. ISSN 1226086X. doi: 10.1016/j.jiec.2009.09.004.

[35] Jiju M. Joseph and C. T. Aravindakumar. Determination of rate constants for the reaction of hydroxyl radicals with some purines and pyrimidines using sunlight. *Journal of Biochemical and Biophysical Methods*, 42(3):115–124, 2000. ISSN 0165022X. doi: 10.1016/S0165-022X(99)00054-8.

[36] T. Schaefer and H. Herrmann. Competition kinetics of OH radical reactions with oxygenated organic compounds in aqueous solution: Rate constants and internal optical absorption effects. *Physical Chemistry Chemical Physics*, 20(16):10939–10948, 2018. ISSN 14639076. doi: 10.1039/c7cp08571k.

[37] M. Erben-Russ, Christa Michel, W. Bors, and M. Saran. Determination of sulfite radical (SO3•-) reaction rate constants by means of competition kinetics. *Radiation and Environmental Biophysics*, 26(4):289–294, 1987. ISSN 0301634X. doi: 10.1007/BF01221974.

[38] Daisuke Minakata, Ke Li, Paul Westerhoff, and John Crittenden. Development of a group contribution method to predict aqueous phase hydroxyl radical (HO•) reaction rate constants. *Environmental Science and Technology*, 43(16):6220–6227, 2009. ISSN 0013936X. doi: 10.1021/es900956c.

[39] B. A. Wols and C. H.M. Hofman-Caris. Review of photochemical reaction constants of organic micropollutants required for UV advanced oxidation processes in water. *Water Research*, 46(9):2815–2827, 2012. ISSN 18792448. doi: 10.1016/j.watres.2012.03.036. URL `http://dx.doi.org/10.1016/j.watres.2012.03.036`.

[40] C. Daniel Harris. *Quantitative Chemical Analysis*. W. H. Freeman and Company, 9 edition, 2016. ISBN 9781464175633.

[41] DIN Forsyning. Drikkevandskvalitet, 2019. URL `https://dinforsyning.dk/da-dk/drikkevand/drikkevandskvalitet`.

[42] GEUS Jupiter. TREFOR Vand, Staurbyskov Vandværk, 2020. URL `https://data.geus.dk/JupiterWWW/vandanalyse.jsp?anlaegid=81663`.

[43] GEUS Jupiter. Hvidovre Vandværk, 2020. URL `https://data.geus.dk/JupiterWWW/vandanalyse.jsp?anlaegid=106361`.

[44] James R. Bolton and Mihaela I. Stefan. Fundamental photochemical approach to the concepts of fluence (UV dose) and electrical energy efficiency in photochemical degradation reactions. *Research on Chemical Intermediates*, 28(7-9):857–870, 2002. ISSN 09226168. doi: 10.1163/156856702604694 74.

[45] David B. Miklos, Christian Remy, Martin Jekel, Karl G. Linden, Jörg E. Drewes, and Uwe Hübner. Evaluation of advanced oxidation processes for water and wastewater treatment – A critical review. *Water Research*, 139: 118–131, 2018. ISSN 18792448. doi: 10.1016/j.watres.2018.03.042.